interaction with heat shock proteins (HSPs). It is reported that the HSPs bind to LOX-1 in endothelial cells, epithelial cells, and antigen-presenting cells (APC) [12,13]. Considering important roles of the HSPs in host-defense system or stress response, the clarification of their interaction of with LOX-1 provides an important insight into the understanding pathogenesis of various inflammatory diseases.

3. HSPs and human diseases

HSPs work as chaperone to affect protein folding of newly synthesized or denatured proteins. The family of HSPs is organized by molecular sizes and functional classes, and it is composed of the HSP100, hsp90, Hsp70, Hsp60, Hsp40, and small heat shock protein families. The HSPs are expressed both constitutively and under stressful conditions, and their expression of HSPs is dynamically regulated. In addition to heat shock, various physiological and pathophysiological stimuli induce a marked increase in the HSPs as the result of such stress as ischemia, oxidative stress, hypoxia, reperfusion, glucose deprivation, or exposure to toxin. The principle role of HSPs is cytoprotection against such stress conditions.

The dysregulation of HSPs is likely associated with various diseases, including cardiovascular diseases, neurodegenerative disorders, and inflammation diseases. It is reported that some HSPs are dynamically up-regulated in atherosclerotic vessels. For example, Xu et al. demonstrated that the intensity of HSP60 expression correlated positively with the severity of atherosclerosis [14]. Furthermore, it is reported that the stress-inducible form of HSP70 was correlated with the development of Apo E-deficient mice [15]. Recently, it is reported that comparative two-dimensional electrophoretic analysis on carotid atherectomy specimens revealed that the expression of HSP27 is increased in the normal-appearing vessels compared with the plaque core [16]. This result suggests that the up-regulated HSP27 was involved in the early stage of atherosclerosis. It is well known that under the ischemic conditions, the up-regulated HSPs exert cytoprotective effects. Indeed, it is reported that the gene transfer HSP70 could preserve ventricular function under the ischemic-reperfusion injury [17]. Conversely, the deletion of the HSP70 gene deteriorates the ischemic area in cerebral infarction in mice [18]. The aggregates of misfolded proteins are observed in a number of neurodegenerative disorders, including Huntington disease, Parkinson disease, and Alzheimer disease. Various investigations demonstrated that the overexpression of HSPs suppressed the formation of aggregates in these pathological conditions. Thus, the intracellular HSPs play a pivotal role in the protection against these diseases.

The HSPs are traditionally regarded as intracellular protein; however, besides the intracellular role, there are reports indicating that some HSP acts as an intercellular signaling molecule since they activate the intracellular signaling system. There are evidences that elevated levels of antibodies against HSP70 in patients with autoimmune diseases [19]. This finding indicates that some HSPs exists in the extracellular milieu. Interestingly, the serum levels of HSP27 correlate with HSP70 and C-reactive protein [16]. Thus, the serum levels of HSPs might be associated with the disease activity or the state of inflammation. Very recently, it is reported that circulating HSP60 in the blood may be a determinant of endothelial dysfunction [20]. However, their cause–result relationships is obscure, that is, it is still unknown whether the increased levels of HSPs in extracellular spaces lead to the disease, or the releases of HSPs from the damaged or injured cells in the active pathological conditions results in the increased levels in the blood stream.

4. Extracellular HSPs and their receptors

These clinical investigations above mentioned rise to the question whether HSPs in the extracellular milieu work as a cytokine and function as a local modulator. If so, the specific receptor for HSPs should exist. Indeed, it is shown that HSP70 selectively bind to some cell types, including natural killer cells dendritic cells, macrophages, peripheral blood cells. Previous investigations reported that HSPs induced a wide variety of inflammatory responses such as production of pro-inflammatory cytokines and via CD14/Toll like receptor (TLR) 2 or 4 [21]. Furthermore, the HSPs exogenously administered possess the activities of HSP. From this viewpoint, chaperokine is referred as such activity of the HSPs, whereas there is some debate with regard to the cytokine activity of extracellular HSPs. It is pointed out that some of these cytokine-effects may be due to contamination of lipopolysaccharide. Nonetheless, there are accumulating evidences that HSPs work in the extracellular spaces. The 'work place' of HSPs is not only intracellular, but also the extracellular space.

So far, several receptors have been proposed as HSP receptors including Toll-like receptor 1 and 4 with their cofactor CD14, CD36, low-density lipoprotein-related protein CD91, SRA, and LOX-1. Thus, several scavenger receptors may work as a HSP receptor. Calderwood et al. examined the relative binding affinity of exogenous HSPs to various receptors, including LOX-1, TLR2, TLR4, and LRP/CD91 [12]. Among these receptors, LOX-1 has the highest affinity to HSP70. Furthermore, they demonstrated that HSP70 binds to human umbilical endothelial cells (HUVEC). However, the LOX-1 blocking antibody did not suppress the HSP70 to HUVEC, whereas this antibody blocked the binding of HSP70 to LOX-1-expressing CHO cells. Thus, LOX-1 is one of potent receptors for the HSP; however, other undermined receptor should be involved in the interaction of HSP to endothelial cells.

5. LOX-1 as receptor for HSP and cross-presentation of antigen

The antigen-presenting cells such as dendritic cells plays a crucial role at the interface between innate and adaptive

immunity. LOX-1 is expressed on dendritic cells and involved in antigen cross-presentation [13]. Cross-presentation is a process by which some exogenous molecules such as HSP are endocytosed by APC via specific receptors, gain access to the MHC class I pathway, and stimulate CD8+ cytotoxic T cells. Cell lysis following injury or infection releases a number of intracellular protein including HSPs into extracellular space. Under certain situations, the HSPs released into extracellular environment form a complex with intracellular peptides. In case of tumor, the HSP-intracellular peptide complexes are recognized by component of immune system, which leads to antitumor immunity. Delneste reported that targeting tumor antigen to LOX-1 *in vivo* induces the development of a protective antitumor CD8+ T cell response [13]. Thus, LOX-1 might be one of targets for cancer immunotherapy.

6. Conclusion

LOX-1 was originally identified as a receptor of oxidized LDL in the endothelial cells. However, progress in the research of LOX-1 has revealed its diverse functions. Among wide variety of biological activities, LOX-1 functions as a receptor of the HSPs. Considering the potent and wide variety of extracellular HSPs, more understanding the interaction of LOX-1 and HSPs provides a novel potential therapeutic strategy for various human diseases.

References

[1] T. Sawamura, N. Kume, T. Aoyama, H. Moriwaki, H. Hoshikawa, Y. Aiba, T. Tanaka, S. Miwa, Y. Katsura, T. Kita, T. Masaki, Nature 386 (1997) 73–77.
[2] D. Li, J.L. Mehta, Circulation 101 (2000) 2889–2895.
[3] L. Cominacini, A. Rigoni, A.F. Pasini, U. Garbin, A. Davoli, M. Campagnola, A.M. Pastorino, V. Lo Cascio, T. Sawamura, J. Biol. Chem. 276 (2001) 13750–13755.
[4] M. Chen, M. Kakutani, M. Minami, H. Kataoka, N. Kume, S. Narumiya, T. Kita, T. Masaki, T. Sawamura, Arterioscler. Thromb. Vasc. Biol. 20 (2000) 1107–1115.
[5] M. Nagase, S. Kaname, T. Nagase, G. Wang, K. Ando, T. Sawamura, T. Fujita, J. Am. Soc. Nephrol. 11 (2000) 1826–1836.
[6] T. Aoyama, T. Sawamura, Y. Furutanai, R. Matsumoto, M.C. Yoshisda, H. Fujiwara, T. Masaki, Biochem. J. 339 (1999) 177–184.
[7] I. Ohki, T. Ishigaki, T. Oyama, S. Matsunaga, Q. Xie, M. Ohnishi-Kameyama, T. Murata, D. Tsuchiya, S. Machida, K. Morikawa, S. Tate, Structure 13 (2005) 905–917.
[8] K. Inoue, Y. Arai, H. Kurihara, T. Kita, T. Sawamura, Circ. Res. 97 (2005) 176–184.
[9] K. Oka, T. Sawamura, K. Kikuta, S. Itokawa, N. Kume, T. Kita, T. Masaki, Proc. Natl. Acad. Sci. USA 95 (1998) 9535–9540.
[10] T. Jono, A. Miyazaki, R. Nagai, T. Sawamura, T. Kitamura, S. Horiuchi, FEBS Lett. 511 (2002) 170–174.
[11] M. Honjo, K. Nakamura, K. Yamashiro, J. Kiry, H. Tanihara, LM. McEvoy, Y. Honda, E.C. Butcher, T. Masaki, Proc. Natl. Acad. Sci. USA 100 (2003) 1274–1279.
[12] J.R. Theriaulta, S.S. Mambula, T. Sawamura, M. Stevensona, S.K. Calderwood, FEBS Lett. 579 (2005) 1951–1960.
[13] Y. Delneste, G. Magistrelli, J. Gauchat, J. Haeuw, J. Aubry, K. Nakamura, N. Kawakami-Honda, L. Goetsch, T. Sawamura, J. Bonnefoy, P. Jeannin, Immunity 17 (2002) 353–362.
[14] Q. Xu, R. Kleindienst, W. Waitz, H. Dietrich, G. Wick, J. Clin. Invest. 91 (1993) 2693–2702.
[15] R.K. Kanwar, J.R. Kanwar, D. Wang, D.J. Ormrod, G.W. Krissansen, Arterioscler. Thromb. Vasc. Biol. 21 (2001) 1991–1997.
[16] H.K. Park, E.C. Park, S.W. Bae, M.Y. Park, S.W. Kim, H.S. Yoo, M. Tudev, Y.H. Ko, Y.H. Choi, S. Kim, D.I. Kim, Y.W. Kim, B.B. Lee, J.B. Yoon, J.E. Park, Circulation 114 (2006) 886–893.
[17] J. Jayakumar, K. Suzuki, I.A. Sammut, R.T. Smolenski, M. Khan, N. Latif, H. Abunasra, B. Murtuza, M. Amrani, M.H. Yacoub, Circulation 104 (2001) 303–307.
[18] S.H. Lee, M. Kim, B.W. Yoon, Y.J. Kim, S.J. Ma, J.K. Roh, J.S. Lee, J.S. Seo, Stroke 32 (2001) 2905–2912.
[19] S. Minota, B. Cameron, W.J. Welch, J.B. Winfield, J. Exp. Med. 168 (1988) 1475–1480.
[20] J.P.J. Halcox, J. Deanfield, A. Shamaei-Tousi, B. Henderson, A. Steptoe, A.R.M. Coates, A. Singhal, A. Lucas, Arterioscler. Thromb. Vasc. Biol. 25 (2005) 141–142.
[21] A. Asea, M. Rehli, E. Kabingu, J.A. Boch, O. Bare, P.E. Auron, M.A. Stevenson, S.K. Calderwood, J. Biol. Chem. 277 (2002) 15028–15034.

ELSEVIER

Cardiovascular Research 76 (2007) 292–302

Cardiovascular Research

www.elsevier.com/locate/cardiores

LOX-1 deletion alters signals of myocardial remodeling immediately after ischemia–reperfusion

Changping Hu [a,b,1], Abhijit Dandapat [a,1], Jiawei Chen [a], Yoshiko Fujita [c], Nobutaka Inoue [c], Yosuke Kawase [d], Kou-ichi Jishage [d], Hiroshi Suzuki [e,f], Tatsuya Sawamura [c], Jawahar L. Mehta [a,*]

[a] *Department of Internal Medicine, University of Arkansas for Medical Sciences and Central Arkansas Veterans Healthcare System, Little Rock, AR, USA*
[b] *Department of Pharmacology, School of Pharmaceutical Sciences, Central South University, Changsha, China*
[c] *Department of Vascular Physiology, National Cardiovascular Center Research Institute, Suita, Osaka, Japan*
[d] *Chugai Research Institute For Medical Science, Inc., Gotenba, Shizuoka, Japan*
[e] *Research Unit for Functional Genomics, National Research Center for Protozoan Diseases, Obihiro University of Agriculture and Veterinary Medicine, Obihiro, Hokkaido, Japan*
[f] *Department of Developmental and Medical Technology, Graduate School of Medicine, University of Tokyo, Tokyo, Japan*

Received 10 April 2007; received in revised form 26 May 2007; accepted 11 July 2007
Available online 18 July 2007
Time for primary review 29 days

Abstract

Objective: Chronic ischemia is associated with alterations in genes that result in myocardial remodeling. An important biochemical basis of cardiac remodeling is generation of reactive oxygen species (ROS). A few studies have suggested that acute ischemia triggers signals for remodeling. We examined the hypothesis that targeted deletion of lectin-like oxidized-LDL receptor (LOX-1) may inhibit signals related to cardiac remodeling.

Methods and results: We generated LOX-1 knockout (KO) mice on C57BL/6 (wild-type mice) background, and subjected wild-type and KO mice to ischemia–reperfusion (I–R). The wild-type mice developed a marked reduction in left ventricular systolic pressure and $\pm dp/dt_{max}$ and an increase in left ventricular end-diastolic pressure following I–R, and this change was much less in the LOX-1 KO mice, indicating preservation of left ventricular function with LOX-1 deletion. There was evidence for marked oxidative stress (NADPH oxidase expression, malondialdehyde and 8-isoprostane) following I–R in the wild-type mice, much less so in the LOX-1 KO mice ($P<0.01$). In concert, collagen deposition (Masson's trichrome and Picro-sirius red staining) increased dramatically in the wild-type mice, but only half as much in the LOX-1 KO mice ($P<0.01$). Collagen staining data was corroborated with procollagen-I expression. Further, fibronectin and osteopontin expression increased in the wild-type mice, but to a much smaller extent in the LOX-1 KO mice ($P<0.01$).

Conclusions: These findings provide compelling evidence that LOX-1 is a key modulator of cardiac remodeling which starts immediately following I–R.

Keywords: Remodeling; Ischemia; Reperfusion; NADPH oxidase; Extracellular matrix

1. Introduction

Heart failure is often the end result of cardiovascular disease states, such as myocardial ischemia [1]. Heart failure is characterized by abundant accumulation of extracellular matrix (ECM) proteins in the extracellular space. Among the ECM proteins, collagens constitute up to 85% [2,3]. Collagen type I is usually present in the form of thick fibres

* Corresponding author. University of Arkansas for Medical Sciences, 4301 West Markham St., Slot 532, Little Rock, AR 72205-7199, USA. Tel.: +1 501 296 1401; fax: +1 501 686 8319.
E-mail address: mehtajl@uams.edu (J.L. Mehta).
[1] These two authors contributed equally.

0008-6363/$ - see front matter © 2007 European Society of Cardiology. Published by Elsevier B.V.
doi:10.1016/j.cardiores.2007.07.003

with a high tensile strength, and is considered a major determinant of myocardial stiffness [3,4]. Fibroblasts are the major source of collagen-I in the myocardium [3,5]. Proliferation of cardiac fibroblasts and deposition of collagen are directly associated with both systolic and diastolic, especially the latter, heart failure [6].

Collagen accumulation in the heart depends not only on its production, but also on its degradation by proteinases, such as matrix metalloproteinase (MMP-2, MMP-3 and MMP-9) [3]. Experimental studies suggest that reactive oxygen species (ROS) released in the early stages of ischemia–reperfusion (I–R) play a major role in the activation of MMPs, and that NADPH oxidase activation, a major source of ROS in the ischemic heart, is a key event in this process [7,8]. Release of cytokines and activation of renin–angiotensin system resulting in the formation of angiotensin II (Ang II) during acute ischemia are also associated with release of ROS and changes in collagens and MMPs [9,10].

Many investigators have highlighted the importance of matricellular protein osteopontin as a key mediator in the cardiovascular system, specifically in vascular remodeling, vascular calcification and left ventricular remodeling [11–13]. Recently, it has been shown that an osteopontin-NADPH oxidase signaling cascade promotes MMP-9 activation [14].

LOX-1 is a lectin-like oxidized-LDL receptor [15]. In previous studies, we showed that LOX-1 is involved in the genesis of oxidant stress and inflammation during myocardial I–R [16,17]. LOX-1 can also act as an adhesion molecule for inflammatory cells [18]. In other studies, we showed that insertion of LOX-1 plasmids in cardiac fibroblasts that are naturally low expressers of LOX-1 alters the biology of fibroblasts to pro-inflammatory phenotype [19]. Further oxidized-LDL treatment enhances collagen formation in fibroblasts that can be blocked by a LOX-1 antibody. These observations collectively suggest that LOX-1 may be an important player in myocardial I–R injury not only by inducing oxidative stress, but also by inducing signals for collagen and MMPs in the ischemic tissues.

We hypothesized that LOX-1 deletion would, by altering the major mediator of myocardial I–R injury, i.e. oxidant stress, improve cardiac diastolic function during ischemia–reperfusion. In addition, it would block or reduce the signal for myocardial remodeling process. Our findings in LOX-1 knockout (KO) mice reveal that "taking away" LOX-1 indeed limits early cardiac remodeling signal following I–R, and this effect is mediated by inhibition of NADPH oxidase.

2. Methods

C57BL/6 mice (also referred to as wild-type mice) were originally obtained from Jackson Laboratories. The homozygous LOX-1 KO mice were developed as described recently [20], and backcrossed 8 times with C57BL/6 strain to replace the genetic background. C57BL/6 and homozygous LOX-1 KO (on C57BL/6 background) mice were bred by brother-sister mating and housed in the breeding colony at University of Arkansas for Medical Sciences, Little Rock, Arkansas. This investigation conforms with the Guide for the Care and Use of Laboratory Animals published by the US National Institutes of Health (NIH Publication No. 85-23, revised 1996). Male mice were utilized in the present studies at 8–10 weeks of age. All experimental procedures were performed in accordance with protocols approved by the Institutional Animal Care and Usage Committee.

2.1. PCR analysis of LOX-1 expression

Wild-type and LOX-1 KO mice were killed with CO_2 anesthesia, and blood, aorta and heart tissues were collected. Genomic DNA was obtained using DNAzol® Reagents (Invitrogen). PCR analysis of genomic DNA was done with the primer pair for deleted portion of LOX-1 gene: 5′-ggccaaccatggctatgggagaatgg-3′ and 5′-cagcgaacacagctccgtcttgaagg-3′, and for neomycin resistant gene: 5′-cgtttccgctgt caccgg-3′ and 5′-caacgctatgtcctgatagcggtcc-3′. 30 cycles of PCR were performed at 94 °C for 40 s, 60 °C for 1 min and 72 °C for 1 min. PCR-amplified products were visualized by ultraviolet light following electrophoresis in 1.5% agarose gel containing ethidium bromide.

2.2. Immunofluorescence staining

The expression of LOX-1 protein and the uptake of ox-LDL were analyzed using immunofluorescence staining. The cryothin sections of aorta were treated with Cy3-labeled anti-mouse LOX-1 monoclonal antibody (1 μg/ml, TS58). Thoracic aortas were incubated for 12 hours at 37 °C in DMEM/10% FCS containing 10 μg/ml DiI-labeled oxidized LDL which was prepared as described previously [21], then washed with PBS three times and snap frozen. To confirm the presence of endothelium, immunostaining with anti-von Willebrand factor, biotinylated anti-CD31 and avidin-FITC was performed, and subjected to observation under a laser confocal microscope.

2.3. Myocardial ischemia–reperfusion protocol

Animals were anesthetized with sodium pentobarbital (60 mg/kg, IP). Anesthesia was maintained via supplemental doses of sodium pentobarbital (30 mg/kg, IP) as needed. Mice were mechanically ventilated with room air using a Harvard respirator (model 683). The respirator's tidal volume was set at 1.4 ml/min and the rate at 110 strokes/min. Electrocardiographic leads were connected to the chest and limbs for continuous monitoring throughout the experiment.

After equilibration period of 10 min, a left thoracotomy was performed in the fourth intercostal space and the pericardium opened to expose the heart. A 6-0 silk suture was passed around the left coronary artery at a point two thirds of the way between its origin near the pulmonary conus and the cardiac apex and a snare was formed by passing both ends of the suture through a piece of polyethylene tubing. Occlusion of the

coronary artery, by clamping the snare against the surface of the heart, caused an area of epicardial cyanosis with regional hypokinesis and ECG changes. Reperfusion was achieved by releasing the snare and was confirmed by conspicuous hyperemic blushing of the previously ischemic myocardium and gradual resolution of the changes in the ECG signal. Another group of animals underwent the same procedure but without ligation of the coronary artery.

The chest wall was approximated and covered with Parafilm wax paper to prevent desiccation. Anesthetized mice were subjected to 60 min of coronary artery occlusion followed by 60 min of reperfusion, except the sham groups.

2.4. Assessment of left ventricular hemodynamics

To assess the hemodynamic status, a 1.4-Fr Millar (SPR-671) pressure transducer catheter was inserted through the right carotid artery into the left ventricle (LV); the position of the catheter was confirmed by typical wave form. Hemodynamic measurements were recorded at baseline and during reperfusion. Analog inputs from the pressure transducer were amplified using a Bridge amplifier and digitized with a PowerLab data-acquisition system (AD Instruments). All parameters were calculated from an average of 30 consecutive beats at each time point. Subsequent off-line evaluations provided LV systolic pressure (LVSP) and LV end-diastolic pressure (LVEDP). The first derivatives of the pressure over time ($\pm dp/dt_{max}$) were calculated from LV pressure tracings as a marker of systolic and diastolic ventricular function, respectively.

Table 1
Primer sequences used for RT-PCR

mRNA	Forward primer	Reverse primer	Annealing temperature (°C)	Size (bp)
$p22^{phox}$	5′-tgg cct gat tct cat cac tgg-3′	5′-ggg aca act cca cag aaa ctc-3′	55	580
$p47^{phox}$	5′-tcc cca gcc agc, act, atg-3′	5′-cag aga tga ccg tgg caa c-3′	56	462
Procollagen-I	5′-tgc ttg cag taa ctt cgt gcc-3′	5′-tgg acc acg ggg acc tgc agg-3′	58	387
MMP-2	5′-tct gcg ggt tct ctg cgt cc-3′	5′-cac ggt ttc agg gtc cag g-3′	55	363
MMP-3	5′-tct tcc ggt cct gct gtg gc-3′	5′-gaa tcc aca ctc tgt ctt ggc-3′	59	389
MMP-9	5′-tcg gct gca gct ctg ctg cc-3′	5′-tca tcg atc atg tct cgc gg-3′	55	376
Fibronectin	5′-ccg gtg gct gtc agt cag a-3′	5′-gtc tca atg gtg gtc tcc tcc-3′	57	368
Osteopontin	5′-tgt ttg gca ttg cct cct cc-3′	5′-cat cga ctg tag gga cga ttg g-3′	56	391
β-actin	5′-ttc tac aat gag gct gcg ttg-3′	5′-cac tgt gtt ggc ata gag gtc-3′	55	560

2.5. Determination of infarct size

At the end of reperfusion, the left coronary artery was re-occluded in the same location as before, and 1 ml 1% Evans blue (Sigma) was injected into the LV cavity and was allowed to perfuse the non-ischemic portions of the heart. The entire heart was excised, weighed, rinsed of excess blue dye, trimmed of right ventricular and atrial tissue, and sliced into 1-mm-thick sections from the apex to base. The slices were incubated in 1% triphenyl tetrazolium chloride (TTC, Sigma) at 37 °C for 15 min to stain the viable myocardium brick red. The slices were then fixed in a 10% formalin solution for 24 h. Each slice was imaged with computer-assisted planimetry (NIH Image J 1.34s) by an observer blinded to sample identity and following parameters was analyzed: (1) area at risk (AAR) as a percent of the left ventricle (LV) (AAR/LV), (2) the infarct area (IA) as a percent of AAR (IA /AAR).

2.6. Determination of oxidant stress in the left ventricular tissues

At the end of reperfusion, entire LV was homogenized in ice-cold 20 mM phosphate buffer. Malondialdehyde (MDA) was measured in the LV homogenate spectrophotometrically and expressed as nmol MDA/g. We also measured 8-iso-prostane, a nonenzymatic metabolite of ROS by enzyme immunoassay (EIA) in the LV homogenates as described previously [22]. The tissue 8-isoprostane level was expressed as ng/g.

2.7. Quantitative analysis of collagen positive area

Paraffin-embedded heart tissues were cut into 5 to 6 sections each 5 μm thick, and the sections were stained with Masson's trichrome and Picro-sirius red. The images were captured by digital imaging system and analyzed with Image pro software (Media Cybernetics). Area positive for collagen was recorded for each section and averaged for each mouse. Data were obtained from at least 3 mice in each group.

2.8. Expression analysis

At the end of reperfusion, entire LV was isolated for the expression analysis of LOX-1, NADPH $p22^{phox}$, NADPH $p47^{phox}$, procollagen-I, MMPs, osteopontin and fibronectin using standard methodologies of RT-PCR and Western blot [9]. Total RNA from the entire LV was extracted using Trizol (Invitrogen). The PCR primers and conditions employed are shown in Table 1. Densities of protein and mRNA bands relative to β-actin were analyzed.

Real-time RT-PCR analysis for the expression of NADPH oxidase ($p22^{phox}$ and $p47^{phox}$ subunits) was performed as described previously [23]. GAPDH was used as a standard control. The primers used are as follows. GAPDH: forward, 5′-AACTTTGGCATTGTGGAAGG-3′;

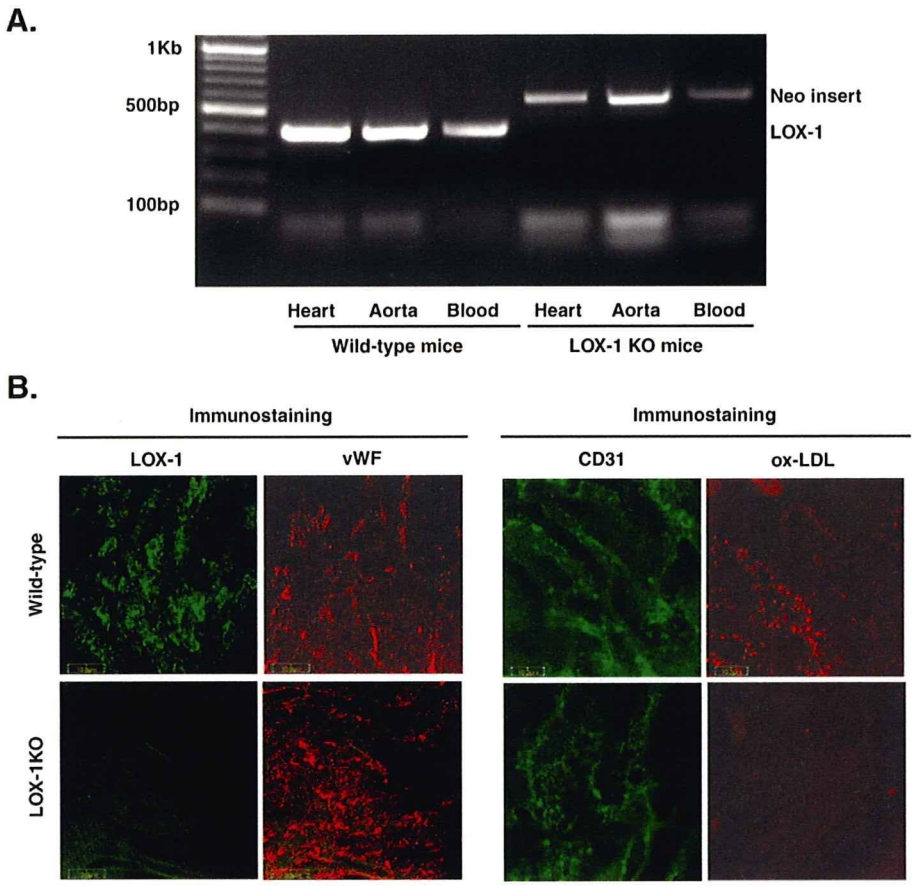

Fig. 1. Evidence for the deletion of LOX-1. (A) PCR analysis of LOX-1 in blood, aorta and heart; (B) Immunofluorescence staining of LOX-1 protein and ox-LDL uptake in aorta.

reverse, 5′-ACACATTGGGGGTAGGAACA-3′. $p22^{phox}$: forward 5′-GCCAACGA GCAGGCGCTGGC-3′; reverse, 5′-CTCGAGGGTATTCCAGCAG-3; $p47^{phox}$: forward, 5-GTGTACATGTTCCTGGTTAAG-3′; reverse, 5′-ATG-GAACTCGTAGATCTCG-3′.

2.9. Statistical analysis

Data are expressed as means±SE. The between-group difference in the infarct size was evaluated by unpaired *t*-test. All hemodynamic values were analyzed with a two-way ANOVA with repeated measures. All other data were analyzed by a two-way ANOVA with a Bonferroni post-hoc test. A $P<0.05$ was considered significant.

3. Results

3.1. Confirmation of LOX-1 deletion

In the genomic DNA from wild-type mice, we amplified a 403 bp LOX-1 fragment by PCR. This fragment was absent in the LOX-1 KO mice tissues. Instead, a neomycin-specific PCR fragment of 564 bp was detected. A representative experiment is shown in the Fig. 1 A. Further, LOX-1 expression was not detected in the vascular tissues of LOX-1 KO mice, although its presence in the endothelium of wild-type mice was confirmed by immunostaining. The endothelial integrity was confirmed by simultaneous staining with von Willebrand factor (Fig. 1 B left). Further, the uptake of ox-LDL in endothelium was undetectable in the LOX-1 KO mice, but clearly seen in the wild-type mice (Fig. 1 B right). These data confirm the genotype of wild-type and LOX-1 KO mice.

3.2. Ischemia–reperfusion induces expression of LOX-1

In keeping with previous studies [16,17], expression of LOX-1 was increased during I–R in the hearts of wild-type mice. The LOX-1 KO mice, as expected, did not show LOX-1 protein at baseline or during I–R (Fig. 2 A).

3.3. Targeted deletion of LOX-1 limits myocardial injury and preserves myocardial function

The basal values of indices of cardiac function (HR, LVSP, LVEDP and $\pm dP/dt_{max}$) were similar in the wild-type and LOX-1 KO mice. In both groups of mice, sham I–R caused no significant change in cardiac function (Table 2).

Following I–R, there was a marked decrease in HR, LVSP, and $\pm dp/dt_{max}$, and a significant increase in LVEDP in the wild-type mice. Reduction in $-dp/dt_{max}$ and increase in

Table 2
Effect of 60-min ischemia followed by 60-min reperfusion on hemodynamic parameters in wild-type and LOX-1 KO mice

	Baseline	Reperfusion time (min)			
		15	30	45	60
Left ventricular systolic pressure (mmHg)					
WT Sham	125±13	130±12	126±11	122±7	123±10
WT I–R	121±8	88±7**	79±10**	59±9**	47±14**
LOX-1 KO Sham	128±8	129±9	127±6	129±7	128±9
LOX-1 KO I–R	124±11	111±9	93±9$^{\#+}$	95±7$^{\#+}$	94±9$^{\#+}$
Left ventricular end-diastolic pressure (mmHg)					
WT Sham	2.2±0.2	2.2±0.4	2.1±0.5	2.2±0.3	2.3±0.5
WT I–R	2.4±0.4	4.2±0.6**	5.5±0.9**	6.9±1.2**	10.4±1.3**
LOX-1 KO Sham	2.1±0.3	2.2±0.5	2.3±0.3	2.2±0.4	2.3±0.4
LOX-1 KO I–R	2.3±0.4	2.8±0.3	3.2±0.7$^{\#+}$	4.0±0.4$^{\#+}$	6.5±1.2$^{\#+}$
$+dp/dt_{max}$ (mmHg/s)					
WT Sham	6889±639	6590±787	6479±323	6689±643	6743±622
WT I–R	6785±645	2765±556**	2832±514**	2249±485**	1824±558**
LOX-1 KO Sham	6708±722	6830±698	6738±470	6484±814	6609±412
LOX-1 KO I–R	5909±433	5012±460$^{\#+}$	4182±554$^{\#+}$	4350±348$^{\#\#++}$	4209±520$^{\#\#++}$
$-dp/dt_{max}$ (mmHg/s)					
WT Sham	6629±615	6539±539	6750±625	6420±361	6509±662
WT I–R	6867±317	2598±151**	2566±136**	1464±213**	1148±164**
LOX-1 KO Sham	6657±559	6761±401	6688±568	6561±598	6239±443
LOX-1 KO I–R	6121±240	5068±321$^{\#+}$	4676±261$^{\#+}$	4330±474$^{\#\#++}$	4038±254$^{\#\#++}$
Heart rate (beats/min)					
WT Sham	484±40	469±48	478±34	473±33	461±39
WT I–R	478±18	259±34**	242±42**	315±15**	327±10**
LOX-1 KO Sham	494±33	477±21	468±17	478±13	496±27
LOX-1 KO I–R	490±13	427±34^{++}	423±19^{++}	430±12^{++}	424±17^{++}

n=4. **P<0.01 vs. WT Sham; $^{\#}P$<0.05, $^{\#\#}P$<0.01 vs. LOX-1 KO Sham;^{+}P<0.05,^{++}P<0.01 vs. WT I–R.
WT-wild-type; I–R-ischemia–reperfusion.

LVEDP indicate diastolic dysfunction. Importantly, despite similar period of I–R in the LOX-1 mice, there was much less deterioration of cardiac function parameters indicating a significant preservation of cardiac function (P<0.01 vs. wild-type mice).

As shown in Fig. 2 B, there were no differences in AAR in the two groups of mice. In the wild-type mice, I–R resulted in extensive infarct (64.1%±10.6% of AAR). In contrast, LOX-1 KO mice had much smaller infarct (21.4%±3.5% of AAR, P<0.01 vs. wild type mice).

3.4. Myocardial ischemia–reperfusion induces oxidative stress

There is release of large amounts of ROS in the early stages of reperfusion, and NADPH oxidase activation is a major source of ROS in this process [7,8]. Release of ROS causes peroxidation of lipids in the heart. We measured MDA, an index of lipid peroxidation, 8-isoprostane, a nonenzymatic metabolite of ROS, and the expression of NADPH oxidase in the mice hearts. As shown in Fig. 2C and D, I–R caused a significant increase in MDA and 8-isoprostane levels in the wild-type mice hearts. In contrast, LOX-1 KO mice hearts had much lower MDA and 8-isoprostane (P<0.01 vs. wild-type mice), indicating much less ROS release. As shown in Fig. 3, both $p22^{phox}$ and $p47^{phox}$ subunits (mRNA and protein) of NADPH oxidase were markedly increased during I–R in both wild-type and LOX-1 KO mice (vs. sham I–R mice), but the LOX-1 KO mice had a much smaller increase (P<0.01 vs. the wild-type mice).

3.5. LOX-1 ablation reduces collagen deposition and MMPs expression

In the wild-type mice, I–R resulted in a marked increase in collagen accumulation (vs. sham I–R mice). In contrast, LOX-1 KO mice had much less collagen accumulation (P<0.01 vs. wild-type mice). The results of Masson's trichrome and Picro-sirius red staining were similar. Representative examples are shown in Fig. 4 (upper left panel), and the summary data are shown in Fig. 4 (lower left panel).

In support of the collagen data, procollagen-I expression (both mRNA and protein) was found to be markedly increased during I–R in the wild-type mice (P<0.01 vs. sham I–R mice), and the increase was much less in the LOX-1 KO despite I–R (Fig. 4, upper and lower right panel). Next,

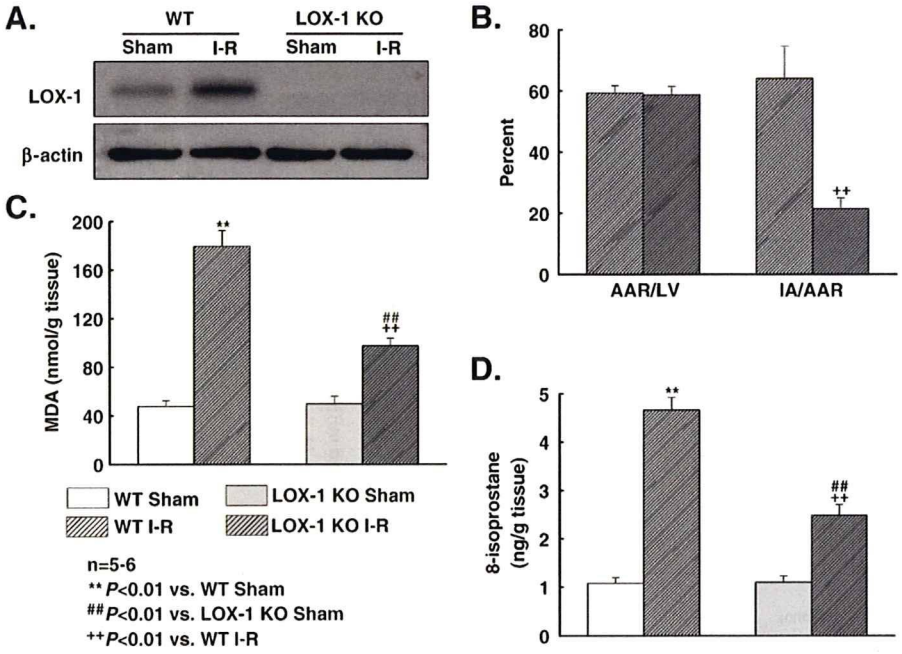

Fig. 2. (A) Western blot analysis of LOX-1 expression in the myocardium; (B) Infarct area (IA) as percent of area at risk (AAR) in different groups of mice; (C) Levels of MDA in the heart tissue; (D) Levels of 8-isoprostane in the heart tissue. WT: wild-type mice; I–R: ischemia–reperfusion.

we determined the expression of MMPs in the heart tissues (Fig. 5). Expression (both mRNA and protein) of MMP-2, MMP-3 and MMP-9 in the wild-type mice was also increased following I–R ($P<0.01$ vs. wild-type mice). It is of note that the basal expression of MMP-2 and MMP-3 was significantly lower in the LOX-1 KO mice than in the wild-type mice. Nonetheless, expression of all three MMPs following I–R remained lower in the LOX-1 KO mice as compared to the wild-type mice.

3.6. LOX-1 ablation attenuates expression of osteopontin and fibronectin

Osteopotin has been shown to interact with fibronectin and plays a role in matrix organization, stability and wound healing [13]. As shown as in Fig. 6, expression (both mRNA and protein) of osteopontin as well as fibronectin increased significantly during I–R in both wild-type and LOX-1 KO mice, but the absolute levels of both remained much lower in the LOX-1 KO mice than in the wild-type mice ($P<0.01$).

4. Discussion

4.1. Summary of main findings

Using state-of-the-art gene knockout technology, we provide convincing evidence that LOX-1 plays a potent role in the induction of myocardial infarct and dysfunction during I–R since the LOX-1 KO mice exhibited a much smaller infarct size and much less cardiac functional deterioration than the wild-type mice despite similar degree of I–R. Importantly, we provide conclusive evidence of expression of remodeling signals following a brief period of I–R in the wild-type mice and attenuation of these signals in the LOX-1 KO mice. The salutary changes in cardiac function in the LOX-1 KO mice were associated with attenuated NADPH oxidase expression, much less ROS release, and decreased collagen deposition.

4.2. Over-expression of collagen-I and metalloproteinases during ischemia–reperfusion

One of the early changes after the onset of ischemia is LV stiffness which persists during chronic ischemia and results in diastolic dysfunction. Although diastolic dysfunction during chronic ischemia has been ascribed to excessive collagen synthesis, enhanced collagen expression 1–2 h after onset of ischemia described in this study is a relatively novel finding. In earlier *in vitro* studies, we found that a brief exposure of cardiac fibroblasts to Ang II results in enhanced collagen-I synthesis [9,24]. We also showed that exposure of cardiac fibroblasts to anoxia-reoxygenation stimulates fibroblast growth as well as collagen type I synthesis and protein expression [25]. Collagen synthesis in response to Ang II and anoxia-reoxygenation was thought to be a response to the release of ROS. In this process, activation of MAP kinases and the redox-sensitive transcription factor NF-κB were noted to play an important role. It is of note that the cytokine TNFα that is released during I–R can also induce collagen synthesis in myofibroblasts [10].

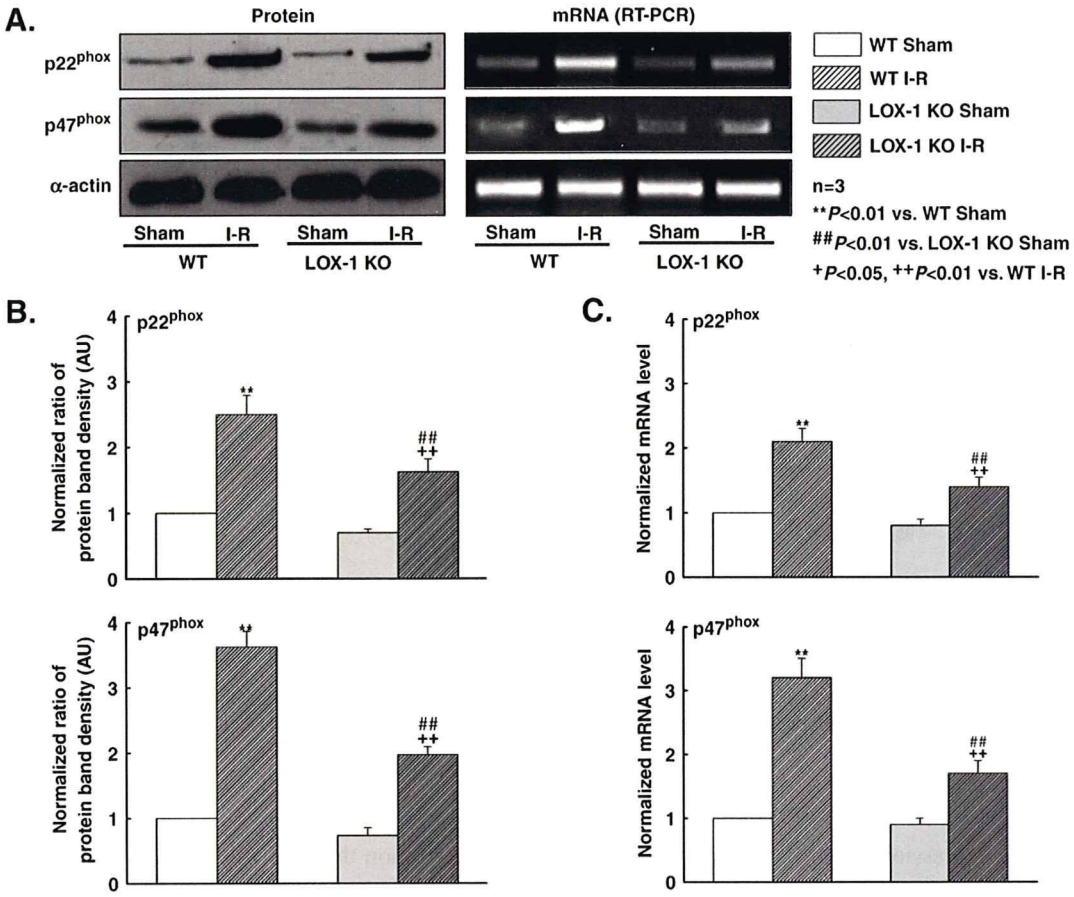

Fig. 3. Expression of NADPH oxidase $p22^{phox}$ and $p47^{phox}$ subunits. (A) Representative protein and mRNA bands determined by Western blot and RT-PCR, respectively; (B) Quantitative protein data; (C) Quantitative mRNA data determined by real time RT-PCR. WT: wild-type mice; I–R: ischemia–reperfusion.

Generally, collagen expression in the heart has been thought to occur several days or weeks after myocardial infarction [26–28]. It is of note that Takino et al [29] showed release of carboxyterminal propeptide of type I procollagen (PICP) in patients with myocardial infarction soon after deployment of reperfusion strategy. Release of PICP peaked at 2–3 weeks after myocardial infarction and correlated with end-diastolic volume. Our observations of increased collagen signals early after I–R are in concordance with the *in vitro* studies from our laboratory [9,24,25] and the *in vivo* study by Takino et al [29].

The marked increase in collagen noted in the present *in vivo* study was found to be associated with release of MMPs (−2, −3 and −9). The release of MMPs early after I–R has been frequently observed in the *in vivo* setting [30], and is thought to contribute to cardiac dilation and rupture during the acute stage of myocardial ischemia. Li et al [16] showed MMP release, expression of adhesion molecules and neutrophil accumulation in the I–R myocardium following a brief period of I–R in the Sprague Dawley rats. *In vitro* studies have also demonstrated that MMP release (by fibroblasts) during exposure of cardiac fibroblasts to anoxia-reoxygenation is triggered by redox-sensitive signals [25].

4.3. Inhibition of collagen-I and MMPs by LOX-1 deletion

Simultaneous release of MMPs and upregulation of collagen expression following I–R suggests that the two processes are inter-related and represent a cellular attempt to regulate the remodeling process. As discussed previously, expression of both MMPs and collagens may be a response to ROS release. Li et al [16] observed that I–R in the rat hearts was associated with over-expression of LOX-1, a finding reproduced in the present study in the wild-type mice. It is of note that LOX-1 activation has been linked to the release of ROS [31]. LOX-1 also acts as an adhesion molecule [18], and this may explain as to why the LOX-1 antibody administration before I–R reduced adhesion molecule expression and neutrophil accumulation in hearts exposed to I–R [16].

We showed that LOX-1 deletion reduces the expression of MMPs and procollagen-I at transcriptional level. We also documented a marked reduction in diastolic function as $-dP/dt_{max}$ fell and LVEDP rose in the wild-type mice subjected to I–R. These alterations may well relate to the increase in collagen signal and deposition in the I–R myocardium. Importantly LOX-1 KO mice had significantly less decline in $-dP/dt_{max}$ and much less increase in LVEDP in concert with a reduction in collagen deposition in the myocardium.

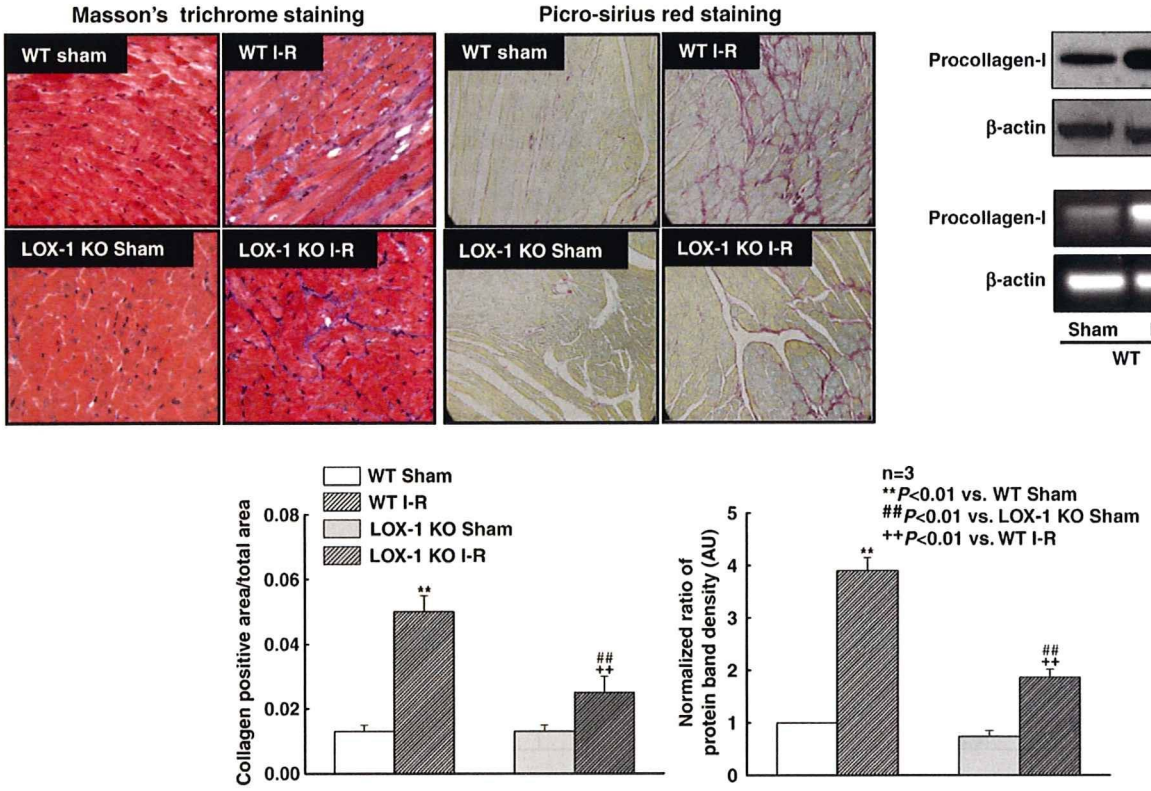

Fig. 4. Collagen and procollagen-I changes following ischemia–reperfusion (I–R). Upper left panel: collagen in representative heart sections (original magnification ×20); Lower left panel: quantitative data on collagen accumulation in heart sections; Upper right panel: representative procollagen-I bands (mRNA and protein); Lower right panel: quantitative data on procollagen-I protein. WT: wild-type mice; I–R: ischemia–reperfusion.

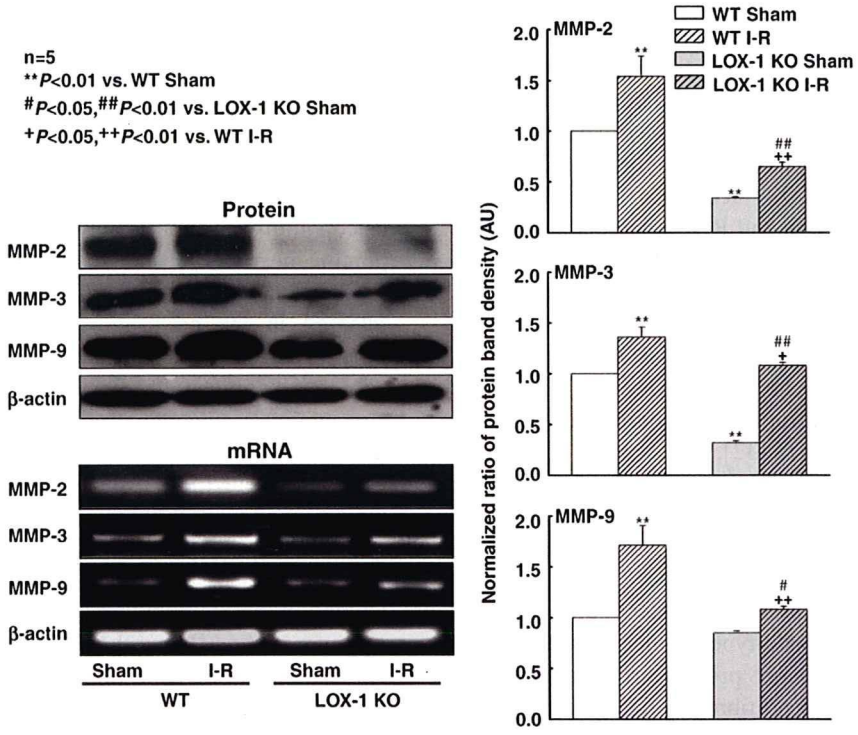

Fig. 5. Expression of matrix metalloproteinases (MMPs) determined by RT-PCR and Western analysis. WT: wild-type mice; I–R: ischemia–reperfusion.

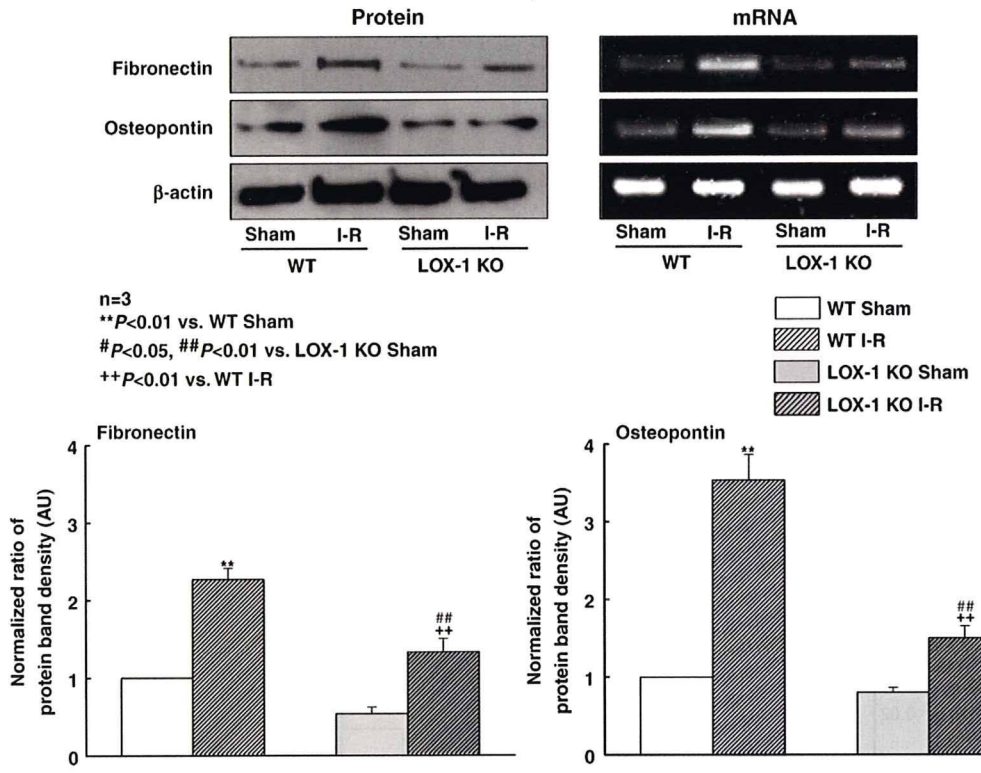

Fig. 6. Expression of fibronectin and osteopontin determined by RT-PCR and Western analysis. WT: wild-type mice; I–R: ischemia–reperfusion.

Reduction in procollagen-I may represent a decrease in oxidant stress in the LOX-1 KO mice. NADPH oxidase is the major source of ROS in the heart [7]. We measured NADPH oxidase expression and the myocardial MDA and 8-isoprostane levels, and found that NADPH oxidase (both $p22^{phox}$ and $p47^{phox}$ subunits) expression and ROS release and resultant lipid peroxidation increased dramatically in the wild-type mice subjected to I–R. This increase in NADPH oxidase and ROS release and resultant lipid peroxidation were much less in the LOX-1 KO mice. The absence of increase in NADPH oxidase and ROS release and resultant lipid peroxidation during I–R in the LOX-1 KO mice is in keeping with a previous report indicating that LOX-1 activation enhances superoxide anion generation [31].

We do not know the exact source of ROS in the present experiments, but it could be cardiomyocytes, fibroblasts, endothelial cell and/or neutrophils. All these cell types have been shown to generate ROS [32].

4.4. Osteopontin and fibronectin expression soon after myocardial ischemia

We observed that the expression of osteopontin as well as fibronectin increased in wild-type mice exposed to I–R. Osteopontin is an adhesion protein implicated as an important mediator of the profibrotic effects of Ang II in the heart. Osteopontin also acts as an adhesion molecule and has been implicated in chemoattraction of monocytes and in cell-mediated immunity [33]. It is also important in smooth muscle migration [34]. The plasma levels of the secreted glycophosphoprotein osteopontin have been associated with the presence and extent of coronary artery disease, especially with coronary calcification and restenosis after coronary intervention [11,12]. In the myocardium exposed to ischemia, osteopontin has been shown to interact with fibronectin suggesting its possible role in matrix organization, stability and wound healing [13]. Kossmehl et al [13] showed that the expression of MMPs, fibronectin and osteopontin was significantly elevated in the infarct area in porcine hearts subjected to 2 h of ischemia and 4 h of reperfusion. Simultaneously, large amounts of PICP were released in the perfusate. Fibroblast-like cells from the infarct area exhibited an enhanced ostepontin and fibronectin expression compared to fibroblasts derived from the control non-infarcted myocardium. Trueblood et al [27] examined the importance of osteopontin in the osteopontin null mice and found that the LV chamber dilation after myocardial infarction was approximately twice as great in osteopontin null mice as in the wild-type mice. Procollagen-I accumulation was also much less in the osteopontin null mice. Collins et al [35] showed that osteopontin is formed in response to Ang II, and the osteopontin null mice had much less cardiac fibroblasts proliferation and much less ECM accumulation after three weeks of Ang II infusion. Interestingly, osteopontin null mice had reduced MMP-2 and MMP-9 activity [36].

The signal for osteopontin expression seems to involve oxidant stress and related pathways. Xie et al [37] showed that p42/44 MAPK is a critical component of the ROS-sensitive signaling pathway activated by Ang II that regulates osteopontin gene expression. In another study in apoE KO mice [38], vitamin E decreased aortic 8-isoprostane and reduced both aortic macrophage infiltration and osteopontin expression. Lai and coworkers [14] demonstrated that osteopontin, via activation of NADPH oxidase-derived superoxide anion formation, promotes upregulation of MMP-9 in primary aortic myofibroblasts and smooth muscle cells under hyperglycemic conditions *in vitro*. Thus, there appears to be a strong link between NADPH oxidase-induced oxidant stress, osteopontin expression and MMP expression and activity. Gorin et al [39] have similarly shown a relationship between NADPH oxidase activation and fibronectin generation in both *in vitro* and *in vivo* conditions. In keeping with these studies, it was not surprising that the expression of osteopontin, fibronectin and MMPs was lower in the hearts of LOX-1 KO mice that had low levels of NADPH oxidase (both $p22^{phox}$ and $p47^{phox}$ subunits) and reduced myocardial 8-isoprostane and MDA content.

4.5. Signal for cardiac remodeling after ischemia–reperfusion

It is now amply evident that a host of mediators are expressed during I–R, including cytokines and Ang II, which account for oxidative stress mostly by activating NADPH oxidase system. The intense oxidant stress, particularly in the infarct-prone region (area at risk), induces upregulation of genes, such as fibronectin, osteopontin, collagen and MMPs soon after ischemia. Enhanced expression of fibronectin, osteopontin and collagen leads to myocardial diastolic dysfunction. Attenuation of the expression of these signals in LOX-1 KO mice suggests that LOX-1 could be a relevant therapeutic target in the management of ischemia-associated myocardial dysfunction.

Acknowledgments

This study was supported by funds from the Department of Veterans Affairs (JLM), a grant from the American Heart Association (PLH), grants from the Ministry of Education, Culture, Sports, Science and Technology of Japan, the Ministry of Health, Labor and Welfare of Japan, the National Institute of Biomedical Innovation, Japan Science and Technology Agency, and the New Energy and Industrial Technology Development Organization (T.S).

References

[1] Wood DA. Preventing clinical heart failure: the rationale and scientific evidence. Heart 2002;88:15–22.
[2] Rekhter MD. Collagen synthesis in atherosclerosis: too much and not enough. Cardiovasc Res 1999;41:376–84.
[3] Heeneman S, Cleutjens JP, Faber BC, Creemers EE, van Suylen RJ, Lutgens E, et al. The dynamic extracellular matrix: intervention strategies during heart failure and atherosclerosis. J Pathol 2003;200:516–25.
[4] Berg TJ, Snorgaard O, Faber J, Torjesen PA, Hildebrandt P, Mehlsen J, et al. Serum levels of advanced glycation end products are associated with left ventricular diastolic function in patients with type 1 diabetes. Diabetes Care 1999;22:1186–90.
[5] Weber KT, Sun Y, Katwa LC, Cleutjens JP, Zhou G. Connective tissue and repair in the heart: potential regulatory mechanisms. Ann N Y Acad Sci 1995;752:286–99.
[6] Weber KT, Brilla CG. Pathological hypertrophy and cardiac interstitium. Fibrosis and renin–angiotensin–aldosterone system. Circulation 1991;83:1849–65.
[7] Hoffmeyer MR, Jones SP, Ross CR, Sharp B, Grisham MB, Laroux FS, et al. Myocardial ischemia/reperfusion injury in NADPH oxidase-deficient mice. Circ Res 2000;87:812–7.
[8] Alfonso-Jaume MA, Bergman MR, Mahimkar R, Cheng S, Jin ZQ, Karliner JS, et al. Cardiac ischemia–reperfusion injury induces matrix metalloproteinase-2 expression through the AP-1 components FosB and JunB. Am J Physiol Heart Circ Physiol 2006;291:H1838–46.
[9] Chen K, Mehta JL, Li D, Joseph L, Joseph J. Transforming growth factor beta receptor endoglin is expressed in cardiac fibroblasts and modulates profibrogenic actions of angiotensin II. Circ Res 2004;95:1167–73.
[10] Theiss AL, Simmons JG, Jobin C, Lund PK. Tumor necrosis factor (TNF) alpha increases collagen accumulation and proliferation in intestinal myofibroblasts via TNF receptor 2. J Biol Chem 2005;280:36099–109.
[11] Kato R, Momiyama Y, Ohmori R, Tanaka N, Taniguchi H, Arakawa K, et al. High plasma levels of osteopontin in patients with restenosis after percutaneous coronary intervention. Arterioscler Thromb Vasc Biol 2006;26:e1–2.
[12] Panda D, Kundu GC, Lee BI, Peri A, Fohl D, Chackalaparampil I, et al. Potential roles of osteopontin and alphaVbeta3 integrin in the development of coronary artery restenosis after angioplasty. Proc Natl Acad Sci U S A 1997;94:9308–13.
[13] Kossmehl P, Schonberger J, Shakibaei M, Faramarzi S, Kurth E, Habighorst B, et al. Increase of fibronectin and osteopontin in porcine hearts following ischemia and reperfusion. J Mol Med 2005;83:626–37.
[14] Lai CF, Seshadri V, Huang K, Shao JS, Cai J, Vattikuti R , et al. An osteopontin–NADPH oxidase signaling cascade promotes pro-matrix metalloproteinase 9 activation in aortic mesenchymal cells. Circ Res 2006;98:1479–89.
[15] Mehta JL, Chen J, Hermonat PL, Romeo F, Novelli G. Lectin-like, oxidized low-density lipoprotein receptor-1 (LOX-1): a critical player in the development of atherosclerosis and related disorders. Cardiovasc Res 2006;69:36–45.
[16] Li D, Williams V, Liu L, Chen H, Sawamura T, Antakli T, et al. LOX-1 inhibition in myocardial ischemia–reperfusion injury: modulation of MMP-1 and inflammation. Am J Physiol Heart Circ Physiol 2002;283: H1795–801.
[17] Li D, Williams V, Liu L, Chen H, Sawamura T, Romeo F, et al. Expression of lectin-like oxidized low-density lipoprotein receptors during ischemia–reperfusion and its role in determination of apoptosis and left ventricular dysfunction. J Am Coll Cardiol 2003;41:1048–55.
[18] Honjo M, Nakamura K, Yamashiro K, Kiryu J, Tanihara H, McEvoy LM, et al. Lectin-like oxidized LDL receptor-1 is a cell-adhesion molecule involved in endotoxin-induced inflammation. Proc Natl Acad Sci U S A 2003;100:1274–9.
[19] Chen K, Chen J, Liu Y, Xie J, Li D, Sawamura T, et al. Adhesion molecule expression in fibroblasts: alteration in fibroblast biology after transfection with LOX-1 plasmids. Hypertension 2005;46:622–7.
[20] Mehta JL, Sanada R, Hu CP, Chen J, Dandapant A, Sugawara F, et al. Deletion of LOX-1 reduces atherogenesis in LDLR knockout mice fed high cholesterol diet. Circ Res 2007;100:1634–42.
[21] Sawamura T, Kume N, Aoyama T, Moriwaki H, Hoshikawa H, Aiba Y, et al. An endothelial receptor for oxidized low-density lipoprotein. Nature 1997;386:73–7.

[22] Oshima Y, Fujio Y, Nakanishi T, Itoh N, Yamamoto Y, Negoro S, et al. STAT3 mediates cardioprotection against ischemia/reperfusion injury through metallothionein induction in the heart. Cardiovasc Res 2005;65:428–35.
[23] Ranganathan G, Unal R, Pokrovskaya I, Yao-Borengasser A, Phanavanh B, Lecka-Czernik B, et al. The lipogenic enzymes DGAT1, FAS, and LPL in adipose tissue: effects of obesity, insulin resistance, and TZD treatment. J Lipid Res 2006;47:2444–50.
[24] Chen K, Chen J, Li D, Zhang X, Mehta JL. Angiotensin II regulation of collagen type I expression in cardiac fibroblasts: modulation by PPAR-gamma ligand pioglitazone. Hypertension 2004;44:655–61.
[25] Chen K, Li D, Zhang X, Hermonat PL, Mehta JL. Anoxia-reoxygenation stimulates collagen type-I and MMP-1 expression in cardiac fibroblasts: modulation by the PPAR-gamma ligand pioglitazone. J Cardiovasc Pharmacol 2004;44:682–7.
[26] Frimm Cde C, Sun Y, Weber KT. Wound healing following myocardial infarction in the rat: role for bradykinin and prostaglandins. J Mol Cell Cardiol 1996;28:1279–85.
[27] Trueblood NA, Xie Z, Communal C, Sam F, Ngoy S, Liaw L, et al. Exaggerated left ventricular dilation and reduced collagen deposition after myocardial infarction in mice lacking osteopontin. Circ Res 2001;88:1080–7.
[28] Maekawa Y, Anzai T, Yoshikawa T, Sugano Y, Mahara K, Kohno T, et al. Effect of granulocyte-macrophage colony-stimulating factor inducer on left ventricular remodeling after acute myocardial infarction. J Am Coll Cardiol 2004;44:1510–20.
[29] Takino T, Nakamura M, Hiramori K. Circulating levels of carboxyterminal propeptide of type I procollagen and left ventricular remodeling after myocardial infarction. Cardiology 1999;91:81–6.
[30] Chen H, Li D, Saldeen T, Mehta JL. TGF-beta 1 attenuates myocardial ischemia–reperfusion injury via inhibition of upregulation of MMP-1. Am J Physiol Heart Circ Physiol 2003;284:H1612–7.
[31] Cominacini L, Rigoni A, Pasini AF, Garbin U, Davoli A, Campagnola M, et al. The binding of oxidized low density lipoprotein (ox-LDL) to ox-LDL receptor-1 reduces the intracellular concentration of nitric oxide in endothelial cells through an increased production of superoxide. J Biol Chem 2001;276:13750–5.
[32] Becker LB. New concepts in reactive oxygen species and cardiovascular reperfusion physiology. Cardiovasc Res 2004;61:461–70.
[33] Ogawa D, Stone JF, Takata Y, Blaschke F, Chu VH, Towler DA, et al. Liver x receptor agonists inhibit cytokine-induced osteopontin expression in macrophages through interference with activator protein-1 signaling pathways. Circ Res 2005;96:e59–67.
[34] Renault MA, Jalvy S, Belloc I, Pasquet S, Sena S, Olive M, et al. AP-1 is involved in UTP-induced osteopontin expression in arterial smooth muscle cells. Circ Res 2003;93:674–81.
[35] Collins AR, Schnee J, Wang W, Kim S, Fishbein MC, Bruemmer D, et al. Osteopontin modulates angiotensin II-induced fibrosis in the intact murine heart. J Am Coll Cardiol 2004;43:1698–705.
[36] Bruemmer D, Collins AR, Noh G, Wang W, Territo M, Arias-Magallona S, et al. Angiotensin II-accelerated atherosclerosis and aneurysm formation is attenuated in osteopontin-deficient mice. J Clin Invest 2003;112:1318–31.
[37] Xie Z, Singh M, Singh K. ERK1/2 and JNKs, but not p38 kinase, are involved in reactive oxygen species-mediated induction of osteopontin gene expression by angiotensin II and interleukin-1beta in adult rat cardiac fibroblasts. J Cell Physiol 2004;198:399–407.
[38] Gavrila D, Li WG, McCormick ML, Thomas M, Daugherty A, Cassis LA, et al. Vitamin E inhibits abdominal aortic aneurysm formation in angiotensin II-infused apolipoprotein E-deficient mice. Arterioscler Thromb Vasc Biol 2005;25:1671–7.
[39] Gorin Y, Block K, Hernandez J, Bhandari B, Wagner B, Barnes JL, et al. Nox4 NAD(P)H oxidase mediates hypertrophy and fibronectin expression in the diabetic kidney. J Biol Chem 2005;280:39616–26.

Scavenger Receptors for Oxidized Lipoprotein in Age-Related Macular Degeneration

Motohiro Kamei,[1] Kazuhito Yoneda,[2] Noriaki Kume,[3] Mihoko Suzuki,[1] Hiroyuki Itabe,[4] Ken-ichi Matsuda,[5] Takeshi Shimaoka,[6] Manabu Minami,[3] Shin Yonehara,[7] Toru Kita,[3] and Shigeru Kinoshita[2]

Purpose. The accumulation of macrophages is known to be involved in the pathogenesis of age-related macular degeneration (AMD), but the reasons why macrophages accumulate in AMD lesions have not been determined. Because the histopathology of AMD has some factors common with those of atherosclerosis, the authors hypothesized that macrophages accumulate to take up oxidized lipoproteins in the eyes of patients with AMD, as has been demonstrated in atherosclerosis.

Methods. Immunohistochemistry was performed on 10 surgically excised choroidal neovascular (CNV) membranes from eyes with AMD. An antibody against oxidized lipoprotein and antibodies against the scavenger receptors SR-PSOX and LOX-1 were used. Antibodies against cytokeratin, CD68, and von Willebrand factor were used to identify retinal pigment epithelium (RPE), macrophages, and vascular endothelial cells, respectively. RT-PCR was performed to detect the mRNAs of the scavenger receptors in the CNV membranes.

Results. Oxidized lipoproteins were immunohistochemically detected in the CNV membranes. Intense immunostaining was observed at the surface of the CNV membranes with the SR-PSOX antibody, whereas LOX-1 immunostaining was weak. Cells expressing scavenger receptors were found to be predominantly macrophages with a minority of RPE. Both SR-PSOX and LOX-1 mRNAs were detected in CNV membranes.

Conclusions. Oxidized lipoproteins are present in AMD lesions. Macrophages and RPE in the CNV membranes express cell surface scavenger receptors for oxidized lipoproteins. These findings suggest that macrophages may accumulate to take up oxidized lipoproteins in AMD and that the control of oxidative stress and macrophage responses may therefore be potential treatments for AMD. (*Invest Ophthalmol Vis Sci.* 2007;48: 1801–1807) DOI:10.1167/iovs.06-0699

Age-related macular degeneration (AMD) is a leading cause of legal blindness in the elderly in the United States[1] and Europe and is rapidly increasing in Asia.[2] Several types of treatments, including photodynamic therapy,[3] anti-VEGF therapy,[4] and macular translocation surgery,[5,6] have been recently developed to treat AMD. However, the pathogenesis of AMD has not been fully understood,[7,8] which results in limited options for current therapies.

AMD is classified into two types: the dry type and the wet type. The wet type of AMD, which is characterized by formation of choroidal neovascular (CNV) membranes, affects 90% of patients with severe visual loss due to AMD. Earlier studies have demonstrated that macrophages accumulate in the tissues of eyes with the wet-type AMD, especially in the CNV membranes.[9–12]. They may play an important role by secreting cytokines and enzymes that induce and enhance neovascularization.[13] In keeping with this idea, the depletion of macrophages reduces CNV formation in an animal model.[14,15] Despite the suggestion that macrophages may play a crucial role in neovascular membrane formation in eyes with AMD, the reason that they accumulate in the AMD lesion remains unknown.

In a histopathological study, Killingsworth et al.[16] observed that macrophages and phospholipid-containing debris were colocalized in Bruch's membrane in eyes with AMD. Curcio et al.[17] also demonstrated an age-related accumulation of cholesterol esters in Bruch's membrane similar to that observed in the arterial intima. These and other studies[18,19] suggest that the histopathology of AMD has some factors common with those of atherosclerosis.

The cellular uptake of oxidized low-density lipoprotein by macrophages and vascular endothelial cells plays a crucial role in the pathogenesis of atherosclerosis.[20] Because the pathologic changes in AMD are similar to those in atherosclerosis[18,19] and atherosclerosis may contribute to the pathogenesis of AMD,[21,22] we hypothesized that macrophages accumulate to take up oxidized lipoproteins in the macular area of eyes with AMD as in the arterial intima in cases with atherosclerosis. To test this hypothesis, we investigated whether oxidized lipoproteins were present in the AMD lesions and whether oxidized lipoprotein-specific cell-surface receptors were expressed in AMD lesions. We also determined what types of cells express those scavenger receptors.

Materials and Methods

Collection and Preparation of CNV Membranes

As a treatment for AMD, choroidal neovascular membranes were surgically excised from 13 eyes of 13 patients with AMD, ages 57 to 80 years (average, 73 years), as descried previously.[23] After an explanation

From the [1]Department of Ophthalmology, Graduate School of Medicine, Osaka University, Suita, Japan; the Departments of [2]Ophthalmology and [5]Anatomy and Neurobiology, Kyoto Prefectural University of Medicine, Kyoto, Japan; the [3]Department of Cardiovascular Medicine, Graduate School of Medicine, and the [7]Graduate School of Biostudies, Kyoto University, Kyoto, Japan; the [4]Department of Biological Chemistry, School of Pharmaceutical Science, Showa University, Tokyo, Japan; and the [6]Molecular Preventive Medicine, Graduate School of Medicine, Tokyo University, Tokyo, Japan.

Presented in part at the annual meeting of the Association for Research in Vision and Ophthalmology, Fort Lauderdale, Florida, April 2004.

Supported by Grant-in-Aid for Scientific Research 15591853 from the Ministry of Education, Science and Culture of Japan.

Submitted for publication June 23, 2006; revised September 12, 2006; accepted February 19, 2007.

Disclosure: **M. Kamei**, None; **K. Yoneda**, None; **N. Kume**, None; **M. Suzuki**, None; **H. Itabe**, None; **K. Matsuda**, None; **T. Shimaoka**, None; **M. Minami**, None; **S. Yonehara**, None; **T. Kita**, None; **S. Kinoshita**, None

The publication costs of this article were defrayed in part by page charge payment. This article must therefore be marked "*advertisement*" in accordance with 18 U.S.C. §1734 solely to indicate this fact.

Corresponding author: Motohiro Kamei, Department of Ophthalmology, E7, Graduate School of Medicine, Osaka University, 2-2 Yamadaoka, Suita, Osaka 565-0871, Japan; mkamei@ophthal.med.osaka-u.ac.jp.

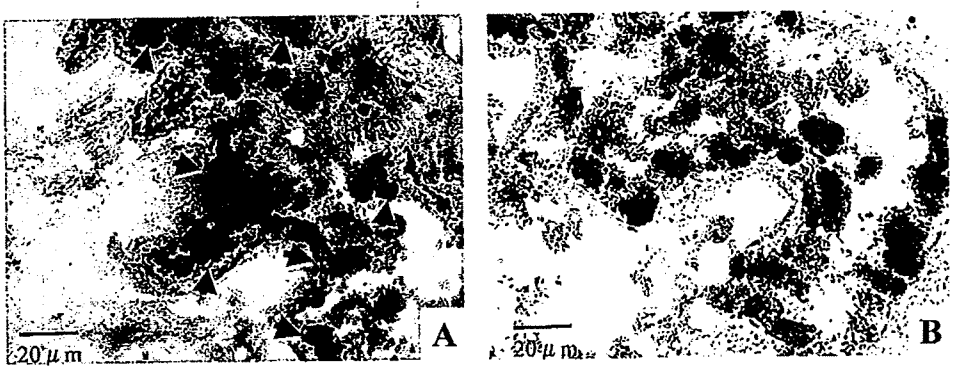

FIGURE 1. Detection of oxidized lipoproteins in choroidal neovascular (CNV) membranes. Photomicrographs of sections from a CNV membrane that was incubated with a monoclonal antibody against oxidized lipoprotein (DLH3) (A) and nonimmune mouse IgM as a negative control (B). Immunostaining of oxidized lipoprotein (*red*) exists in and around the region of autofluorescent pigment granules in CNV membrane (*arrows*). Original magnification, ×20.

of the purpose of the study, an informed consent was obtained from each patient to collect and study the excised tissues. The procedures used to collect and prepare the tissues conformed to the tenets of the Declaration of Helsinki.

Ten of the specimens were used for immunohistochemistry and three for mRNA extraction. For immunohistochemistry, the surgically excised CNV membranes were placed in balanced saline solution in the operating room, kept at 4°C, and embedded in optimum cutting temperature (OCT) compound (Sakura Finetechnical Co, Ltd., Tokyo, Japan) within 2 hours after excision. Cryosections, 8 μm thick, were made for immunohistochemistry. For RT-PCR analysis, the CNV membranes were placed in liquid nitrogen in the operating room immediately after surgical excision and kept at −80°C until RNA extraction.

Immunohistochemistry for Oxidized Lipoproteins

Indirect immunohistochemistry was performed on cryosections of surgically excised membranes with a monoclonal antibody (IgM) against oxidized lipoproteins, FOH1a/DLH3. The antibody was generated by immunizing a mouse against homogenates of human atheroma. It has been found to recognize oxidized phosphatidylcholine as an epitope and has been used for detecting oxidized lipoproteins in atherosclerotic lesions.[24] The avidin-biotin complex immunoperoxidase technique (Vector Laboratories Inc., Burlingame, CA) was used. In brief, after the sections were fixed in cold 4% formaldehyde, the endogenous peroxidase activity was blocked by $NaIO_4$. The specimens were incubated with 0.3% BSA-PBS to block nonspecific immunoreaction and then with DLH3 at a dilution of 1:100, followed by incubation with a biotinylated horse anti-mouse IgM antibody. The sections were then incubated with streptavidin-biotin complex labeled with peroxidase. The immunoreactivity was made visible with 3-amino-9-ethylcarbazole (AEC; Vector Laboratories, Inc.). Sections incubated with nonimmune mouse IgM as a primary antibody served as negative controls.

For further characterization of the positive cells, double staining was performed with DLH3 and anti-CD68 (Zymed, South San Francisco, CA) to detect the distribution of macrophages. After DLH3 staining, the specimens were incubated with anti-CD68 monoclonal antibody at a dilution of 1:100, followed by incubation with a biotinylated horse anti-mouse IgG antibody. The sections were then incubated with ABC-AP reagent (Vectastain; Vector Laboratories, Inc.). The second substrate-chromogen solution (Vector blue; Vector Laboratories, Inc.) was incubated on the slides for 1 to 5 minutes.

Immunohistochemistry for Scavenger Receptors

To identify scavenger receptors and cells expressing these receptors in CNV membranes, double staining was performed with an anti-scavenger receptor antibody and a cell marker antibody. After fixation in cold 4% formaldehyde, the sections were incubated with the primary antibody mixtures including one of the anti-scavenger receptor antibodies and one of the cell markers. Antibodies against scavenger receptors included anti-LOX-1 (lectin-like Ox-LDL receptor-1) monoclonal antibody[19] (1:50 dilution) and anti-SR-PSOX (scavenger receptor that binds phosphatidylserine and oxidized lipoprotein) polyclonal antibody[25] (1:200 dilution). Cell marker monoclonal antibodies included CD68 (1:400 dilution; Zymed), pan cytokeratin (1:500 dilution; Sigma-Aldrich, St. Louis, MO), and von Willebrand factor (vWF; 1:1000 dilution; Dako Co., Glostrup, Denmark). In cases in which the primary antibody mixture contained both monoclonal antibodies (e.g., a mixture of anti-LOX-1 antibody and a cell marker), the primary antibodies were mixed with a labeling kit (Zenon; Invitrogen-Molecular Probes, Inc, Eugene, OR), according to the manufacturer's instruction. The specimens were incubated with the mixture for 1 hour at room temperature and then incubated with secondary antibodies, Alexa Fluor 488–conjugated anti-mouse IgG antibody and Alexa Fluor 546–conjugated anti-rabbit IgG antibody (Invitrogen-Molecular Probes), for 1 hour at room temperature. The specimens were examined with a confocal microscope. For control sections, a mixture of nonimmunized mouse IgG and rabbit IgG was applied as the primary antibody.

The intensity of the immunologic reaction was graded semiquantitatively according to a previous report.[26] The grades for the degree of staining were: none (−), mild (+, up to one third of cells stained), moderate (++, one third to two thirds of cells stained), or heavy (+++, two thirds to all cells stained). The degree of staining of the scavenger receptors was determined by comparing the relative number of positively stained cells to all cells in the section. For each cell marker, the degree of staining was determined by comparing the relative number of double-stained cells that appeared yellow to all cells positively stained with each scavenger receptor antibody.

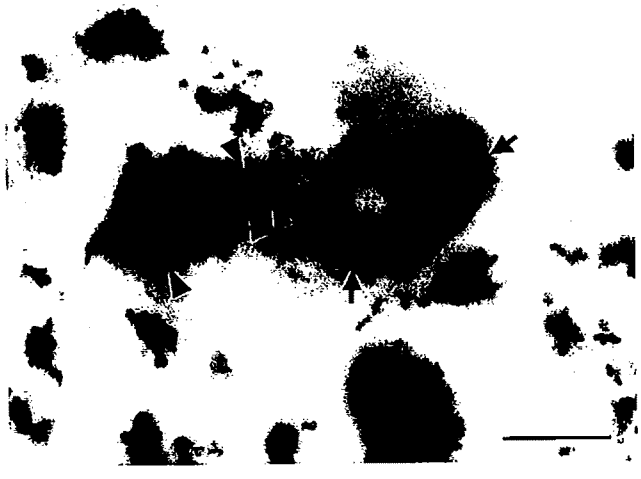

FIGURE 2. Double staining of oxidized lipoproteins and CD68 in CNV membranes. Immunoreactions with the anti-oxidized lipoprotein antibody (*red*) are colocalized with those with anti-CD68 antibody (*blue*: *arrowheads*) as well as pigment granules (*arrows*). These results suggest that oxidized lipoproteins are present in macrophages and RPE cells. Bar, 10 μm. Original magnification, ×630.

TABLE 1. Immunohistochemical Staining for Scavenger Receptors and Rate of Cell Markers in CNV Associated with AMD

Case	Age	Gender	SR-PSOX	CD68	PCK	vWF	LOX-1	CD68	PCK	vWF
1	65	F	+	+++	−	−	+	−	+	−
2	77	F	++	++	−	−	+	++	++	+
3	70	M	+++	+++	−	−	++	++	++	−
4	72	F	+++	+++	−	−	−	NA	NA	NA
5	65	M	+++	+++	+	−	++	+	++	+
6	68	M	+++	+++	−	−	−	NA	NA	NA
7	76	F	+	++	−	−	+	−	+	−
8	71	M	+++	+++	−	−	−	NA	NA	NA
9	69	M	++	+++	−	−	−	NA	NA	NA
10	61	M	+++	+++	−	−	+	−	++	+

The degree of staining of the scavenger receptors was determined by counting the relative number of positively stained cells among all cells in the section. For each cell marker, the degree of staining was determined by counting the relative number of double-stained cells that appeared yellow among all cells positively stained with each scavenger receptor antibody.

Reverse Transcription–Polymerase Chain Reaction

Total cellular RNA was extracted from three CNV membranes (RNeasy Mini Kit; Qiagen, Valencia, CA), and the extracted RNA was reverse transcribed with random primers (Toyobo, Osaka, Japan). The transcribed cDNA was used for polymerase chain reaction amplification with specific primers for LOX-1, SR-PSOX, and GAPDH. The two specific primers used to amplify LOX-1 were 5′-TGCTCTAGAGCACGGCAACAAGCA-3′, and 5′-GGGATCCCGGTGCTCTTAGGTTTGCC-3′; for SR-PSOX 5′-ACTCAGCCAGGCAATGGCAAC-3′, and 5′-GGTATTAGAGTCAGGTGCCAC-3′; and for GAPDH 5′-GGTGAAGGTCGGTGTGAACG-3′ and 5′-CAAAGTTGTCATGGATGACC-3′. PCR amplification was performed by 35 cycles of denaturation, annealing, and elongation with polymerase (TaqDNA; Toyobo). For positive control of each scavenger receptor, total cellular RNA was isolated from a cultured human monocyte cell line, THP-1.[25]

RESULTS

Oxidized Lipoproteins in CNV Membranes

Surgically excised CNV membranes were immunopositive to a monoclonal antibody against oxidized lipoprotein (Fig. 1). Although the surgically excised neovascular tissues contained no retinal components except for RPE cells and did not show the normal tissue structure, immunoreactivity to oxidized-lipoprotein was present mainly in and around the area of the autofluorescent pigment granules. Double staining revealed that immunostaining of oxidized lipoproteins colocalized with the CD68-positive cells as well as cells with pigment granules (Fig. 2), which suggested that oxidized lipoproteins are present on macrophages and RPE cells.

Scavenger Receptors for Oxidized Lipoproteins

SR-PSOX was detected in all CNV membranes. The peripheral regions of the CNV membranes were strongly immunopositive and the membrane stroma mildly immunopositive for SR-PSOX. The distribution of LOX-1 was similar to that of SR-PSOX, but the immunostaining was less intense and was observed in only 6 of 10 samples (Table 1). These results suggest that SR-PSOX was more prominent than LOX-1 in CNV membranes of eyes with AMD.

Cells Expressing Scavenger Receptors for Oxidized Lipoproteins

To identify the cells expressing the scavenger receptors in the CNV membranes, we performed double staining with the cell-marker antibodies CD68, pan cytokeratin, and vWF factor, which stain macrophages, RPE cells, and vascular endothelial cells, respectively.

Merging the double-stained images composed of a section stained with an anti-scavenger receptor antibody and anti-CD68 antibody (Fig. 3) demonstrated that almost all the CD68-positive cells (i.e., macrophages) were SR-PSOX positive, and 60% to 70% of these cells were also LOX-1 positive. In contrast, most SR-PSOX-positive cells and many LOX-1-positive cells were identical with CD68-positive cells (Table 1). These results indicate that most macrophages expressed both scavenger receptors, but predominantly SR-PSOX. Cells expressing these scavenger receptors were mainly macrophages, but CNV membranes had a minor population of LOX-1-positive cells other than macrophages.

In the merged images composed of sections stained with an antiscavenger receptor antibody and anti-pan cytokeratin antibody (Fig. 4), almost all pan-cytokeratin-positive cells (i.e., RPE cells) were SR-PSOX negative, and most were LOX-1 positive. In contrast, most SR-PSOX-positive cells were pan cytokeratin negative, and many LOX-1-positive cells were identical with pan cytokeratin-positive cells (Table 1). These results indicate that almost all RPE cells expressed only LOX-1. Cells expressing SR-PSOX were not the RPE cells, and there were cells other than RPE cells that expressed LOX-1.

Images composed of sections stained with an anti-scavenger receptor antibody and anti-vWF factor antibody demonstrated that almost all the vWF-positive cells (i.e., vascular endothelial cells), were not SR-PSOX-positive, that some of those cells were LOX-1 positive, and that most of the SR-PSOX-positive or LOX-1-positive cells were not vWF-positive (Fig. 5; Table 1). These results indicate that only a limited number of vascular endothelial cells expressed only LOX-1.

Summarizing the double-staining results, cells expressing SR-PSOX were almost exclusively macrophages, and cells expressing LOX-1 were macrophages and RPE cells, with a minority of vascular endothelial cells. Macrophages are the main cell type expressing scavenger receptors for oxidized lipoproteins.

mRNAs of Scavenger Receptors for Oxidized Lipoproteins Expressed in CNV Membrane

To determine whether the mRNAs of scavenger receptors are expressed in human CNV membranes, RT-PCR analyses were performed on total cellular RNA extracted from three surgically excised CNV membranes. The mRNAs of both SR-PSOX and LOX-1 were detected in human CNV membranes (Fig. 6).

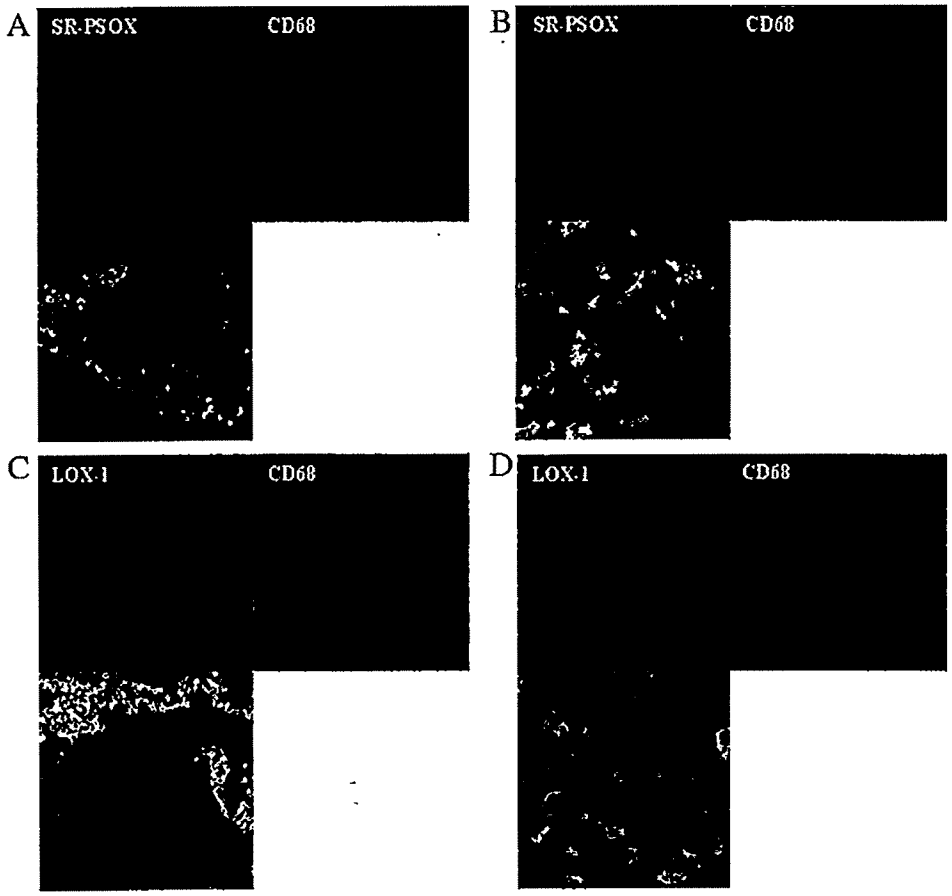

FIGURE 3. Localization of scavenger receptors and macrophages. Images composed of a section stained with anti-SR-PSOX polyclonal antibody (*red*) and another with anti-CD68 monoclonal antibody (*green*), and a merged image (**A, B**) demonstrates that almost all CD68-positive cells were SR-PSOX positive. Serial sections of the CNV membrane were stained with anti-LOX-1 monoclonal antibody (*red*) and anti-CD68 monoclonal antibody (*green*), and a merged image (**C, D**) demonstrates that 60% to 70% of the CD68-positive cells were LOX-1 positive. Most, but not all SR-PSOX- or LOX-1-positive cells were identical with CD68-positive cells. Magnification: (A) ×7; (B, D) ×126; (C) ×14.

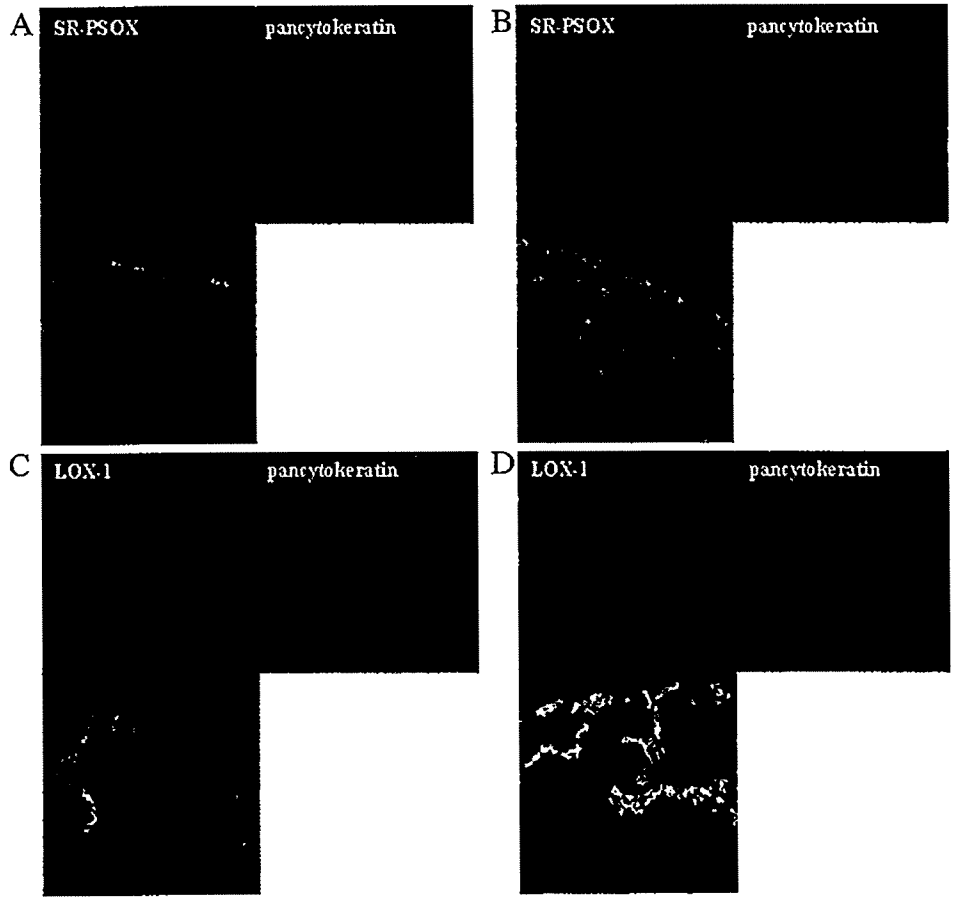

FIGURE 4. Localization of scavenger receptors and retinal pigment epithelium. Images composed of a section stained with anti-SR-PSOX polyclonal antibody (*red*) and anti-pan cytokeratin monoclonal antibody (*green*) and a merged image shows that almost all pan cytokeratin-positive cells were SR-PSOX negative. Serial sections of the CNV membrane stained with anti-LOX-1 monoclonal antibody (*red*) and anti-pan cytokeratin monoclonal antibody (*green*) and a merged image shows that almost all pan cytokeratin-positive cells were LOX-1 positive. Not all LOX-1-positive cells are identical with pan cytokeratin-positive cells. Magnification: (A, C) ×7; (B) ×20; (D) ×40.

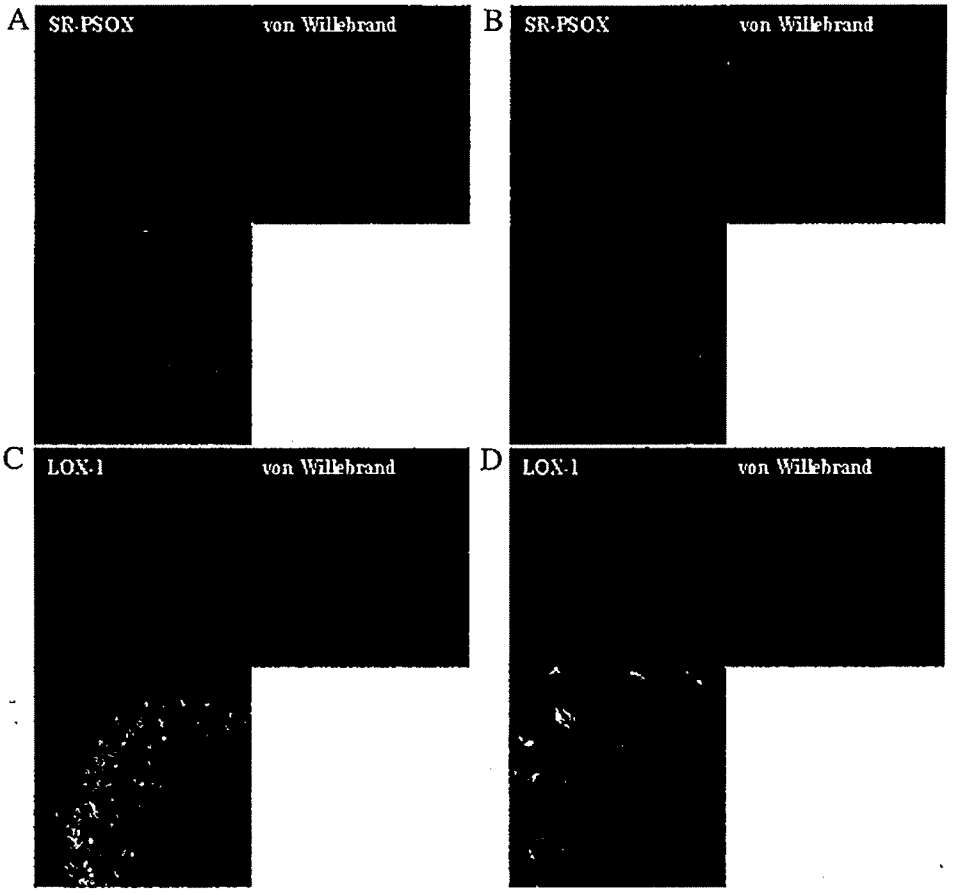

FIGURE 5. Localization of scavenger receptors and vascular endothelium. Images of a section stained with anti-SR-PSOX polyclonal antibody (*red*) and anti-vWF monoclonal antibody (*green*) and a merged image demonstrate that almost all the vWF positive cells were not SR-PSOX positive and that most of the SR-PSOX-positive cells were not vWF positive. Serial sections of the CNV membrane were stained with anti-LOX-1 monoclonal antibody (*red*) and anti-vWF monoclonal antibody (*green*), and a merged image demonstrates that some of the vWF-positive cells were LOX-1 positive and that most of LOX-1 positive cells were not vWF positive. Magnification: (A) ×14; (D) ×30.

DISCUSSION

Because the histopathological changes in AMD are similar to those seen in atherosclerosis,[9–12,16–19] we suspected that scavenger receptors for oxidized lipoproteins might be present in AMD lesions. Our results demonstrated that oxidized lipoproteins and the scavenger receptors for oxidized lipoproteins are colocalized in the CNV membranes of AMD eyes. We had already found that oxidized lipoproteins in the macula increase with age in normal eyes and in AMD eyes, compared with age-matched normal eyes.[27] These findings support our hypothesis that pathogenesis of AMD has some similarities with the pathologic mechanisms of atherosclerosis in which macrophages accumulate to ingest the oxidized low-density lipoprotein by scavenger receptors specific for oxidized lipoproteins at the early stage.

Oxidized lipoproteins were observed in and around the area of the autofluorescent pigment granules and colocalized with RPE cells and macrophages. This finding suggests that oxidized lipoproteins may accumulate in RPE cells and Bruch's membrane, which is consistent with the accumulation of cholesterol esters or phospholipid-containing debris in Bruch's membrane.[17,18] In addition, considering that the antioxidized lipoprotein antibody DLH3 detects foam cells, which take up Ox-LDL in early atherosclerotic lesions,[24] the positive staining may in part indicate oxidized lipoprotein-laden cells, which are possibly RPE cells and macrophages.

Although previous studies demonstrated that macrophages accumulate in AMD lesions,[9–12,16] it is not known why macrophages accumulate in these areas. van der Schaft et al.[28] reported that immune reactions do not appear to be involved in attracting the macrophages in AMD, because distinct immune complexes have not been found in the basal laminar deposits or in drusen. In this study, we found accumulation of oxidized lipoproteins and macrophages that possessed scavenger receptors. Oxidized lipoproteins have been shown to cause inflammatory reactions resulting in the accumulation of macrophages[29–31] in many studies on atherosclerosis, and the

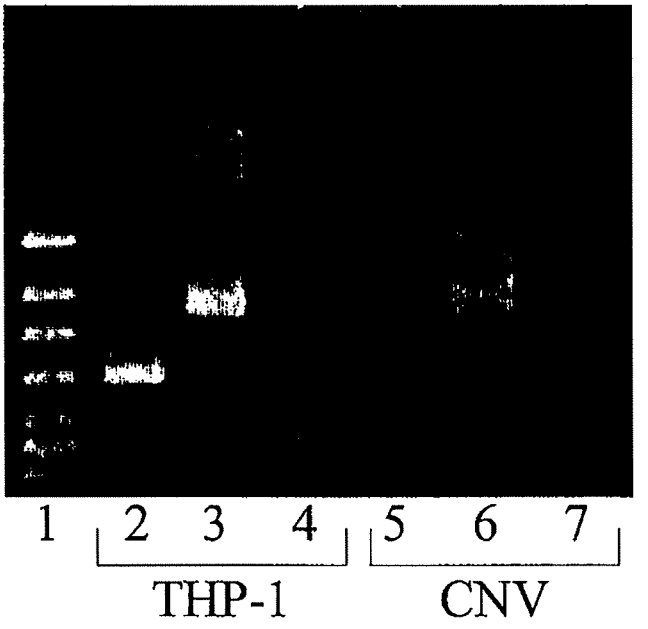

FIGURE 6. Scavenger receptor mRNA were present in CNV membranes. RT-PCR revealed expression of both SR-PSOX mRNA (*lane 6*) and LOX-1 mRNA (*lane 7*) in human CNV membranes. *Lane 1*: molecular marker; *lanes 2* to *4*: positive control; *lanes 5* to *7*: CNV membrane; *lanes 2* and *5*: GAPDH; *lanes 3* and *6*: SR-PSOX; *lanes 4* and *7*: LOX-1.

histopathology of atherosclerosis is similar to that of AMD. Chang et al. reported that oxidized phosphatidylcholine binds to C-reactive protein, an opsonic molecule activating the classic complement pathway and Fc-γ receptor endocytosis of macrophages.[29,30] Complements have also been shown in atherosclerotic plaques together with oxidized lipoprotein, C-reactive proteins, and macrophages.[31] In recent genetic investigations, Hageman et al.[32] reported that a variation in the factor H gene increases the likelihood of development of AMD, and three other studies have demonstrated a linkage of the same gene to AMD.[33-35] These findings suggest that complement–macrophage reaction is involved in the accumulation of macrophage in AMD lesions.

In our study, oxidized lipoproteins and macrophages were colocalized in AMD lesions and most macrophages in the CNV membranes expressed oxidized lipoprotein-specific scavenger receptors. Because the uptake of oxidized LDL by macrophages via scavenger receptors and accumulation of lipid-laden foam cells in the arterial intima are key events in early atherogenesis,[19,20] our findings suggest that macrophages may also accumulate in the area of the AMD, possibly to phagocytose oxidized lipoproteins through scavenger receptors. Furthermore, the expressions of SR-PSOX and LOX-1 are clinically important, because both of them have higher specificity to biologically degenerative LDL and not to artificially degenerative LDL, such as acetylated LDL than do other scavenger receptors.[19,25,36]

In atherosclerosis, the expressions of LOX-1 and SR-PSOX have specific sites. Endothelial cells expresses mainly LOX-1 from the early stage of atherosclerotic plaques, and macrophages and smooth muscle cells express LOX-1 in the advanced stage.[19,36] SR-PSOX is expressed mainly by macrophages,[25] although the relationship between the LOX-1-positive cells and the SR-PSOX-positive cells has not been determined. In this study, SR-PSOX were more prominent than LOX-1 in CNV membranes, cells expressing SR-PSOX were almost exclusively macrophages, and cells expressing LOX-1 were macrophages and RPE cells, with a minority of vascular endothelial cells. A specificity of scavenger receptors may also exist in AMD lesions, which means that SR-PSOX expressed on macrophages may function predominantly. We do not have any evidence of a relationship between the LOX-1-positive RPE and SR-PSOX-positive macrophages.

In conclusion, our results provide new and significant information on the close link between oxidized lipoproteins and macrophages to AMD. Additional studies are needed to evaluate these changes more quantitatively and to clarify the results at the molecular level. Our findings support the suggestion that supplementation with antioxidants, vitamins, and minerals may reduce the risk of development of AMD.[37] Taken together with the results of recent studies demonstrating that macrophage depletion reduced CNV formation in an animal model,[14,15] our findings suggest that suppressing macrophage accumulation by controlling the macrophage responses to oxidative lipoproteins or suppressing phospholipid oxidation may be treatments for AMD.

References

1. Fine SL, Berger JW, Maguire MG, Ho AC. Age-related macular degeneration. *N Engl J Med.* 2000;342:483-492.
2. Miyazaki M, Kiyohara Y, Yoshida A, Iida M, Nose Y, Ishibashi T. The 5-year incidence and risk factors for age-related maculopathy in a general Japanese population: the Hisayama study. *Invest Ophthalmol Vis Sci.* 2005;46:1907-1910.
3. Schmidt-Erfurth U, Miller JW, Sickenberg M, et al. Photodynamic therapy with verteporfin for choroidal neovascularization caused by age-related macular degeneration: results of retreatments in a phase 1 and 2 study. *Arch Ophthalmol.* 1999;117:1177-1187.
4. Eyetech Study Group. Preclinical and phase 1A clinical evaluation of an anti-VEGF pegylated aptamer (EYE001) for the treatment of exudative age-related macular degeneration. *Retina.* 2002;22:143-152.
5. Machemer R. Macular translocation. *Am J Ophthalmol.* 1998;125:698-700.
6. Kamei M, Tano Y, Yasuhara T, Ohji M, Lewis H. Macular translocation with chorioscleral outfolding: 2-year results. *Am J Ophthalmol.* 2004;138:574-581.
7. Zarbin MA. Age-related macular degeneration: review of pathogenesis. *Eur J Ophthalmol.* 1998;8:199-206.
8. Kamei M, Hollyfield JG. TIMP-3 in Bruch's membrane: changes during aging and in age-related macular degeneration. *Invest Ophthalmol Vis Sci.* 1999;40:2367-2375.
9. Grossniklaus HE, Cingle KA, Yoon YD, Ketkar N, L'Hernault N, Brown S. Correlation of histologic 2-dimensional reconstruction and confocal scanning laser microscopic imaging of choroidal neovascularization in eyes with age-related maculopathy. *Arch Ophthalmol.* 2000;118:625-629.
10. Lopez PF, Grossniklaus HE, Lambert HM, et al. Pathologic features of surgically excised subretinal neovascular membranes in age-related macular degeneration. *Am J Ophthalmol.* 1991;112:647-656.
11. Dastgheib K, Green WR. Granulomatous reaction to Bruch's membrane in age-related macular degeneration. *Arch Ophthalmol.* 1994;112:813-818.
12. Grossniklaus HE, Miskala PH, Green WR, et al. Histopathologic and ultrastructural features of surgically excised subfoveal choroidal neovascular lesions: submacular surgery trials report no. 7. *Arch Ophthalmol.* 2005;123:914-921.
13. Oh H, Takagi H, Takagi C, et al. The potential angiogenic role of macrophages in the formation of choroidal neovascular membranes. *Invest Ophthalmol Vis Sci.* 1999;40:1891-1898.
14. Sakurai E, Anand A, Ambati BK, van Rooijen N, Ambati J. Macrophage depletion inhibits experimental choroidal neovascularization. *Invest Ophthalmol Vis Sci.* 2003;44:3578-3585.
15. Espinosa-Heidmann DG, Suner IJ, Marin-Castano ME, Hernandez EP, Pereira-Simon S, Cousins SW. Macrophage depletion diminishes lesion size and severity in experimental choroidal neovascularization. *Invest Ophthalmol Vis Sci.* 2003;44:3586-3592.
16. Killingsworth MC, Sarks JP, Sarks SH. Macrophages related to Bruch's membrane in age-related macular degeneration. *Eye.* 1990;4:613-621.
17. Curcio CA, Millican CL, Bailey T, Kruth HS. Accumulation of cholesterol with age in human Bruch's membrane. *Invest Ophthalmol Vis Sci.* 2001;42:265-274.
18. Mullins RF, Russell SR, Anderson DH, Hageman GS. Drusen associated with aging and age-related macular degeneration contain proteins common to extracellular deposits associated with atherosclerosis, elastosis, amyloidosis, and dense deposit disease. *FASEB J.* 2000;14:835-846.
19. Kataoka H, Kume N, Miyamoto S, et al. Expression of lectinlike oxidized low-density lipoprotein receptor-1 in human atherosclerotic lesions. *Circulation.* 1999;99:3110-3117.
20. Witztum JL, Steinberg D. Role of oxidized low density lipoprotein in atherogenesis. *J Clin Invest.* 1991;88:1785-1792.
21. Friedman E. The role of the atherosclerotic process in the pathogenesis of age-related macular degeneration. *Am J Ophthalmol.* 2000;130:658-663.
22. Vingerling JR, Dielemans I, Bots ML, Hofman A, Grobbee DE, de Jong PT. Age-related macular degeneration is associated with atherosclerosis. The Rotterdam Study. *Am J Epidemiol.* 1995;142:404-409.
23. Sawa M, Kamei M, Ohji M, Motokura M, Saito Y, Tano Y. Changes in fluorescein angiogram early after surgical removal of choroidal neovascularization in age-related macular degeneration. *Graefes Arch Clin Exp Ophthalmol.* 2002;240:12-16.
24. Itabe H, Takeshima E, Iwasaki H, et al. A monoclonal antibody against oxidized lipoprotein recognizes foam cells in atherosclerotic lesions: complex formation of oxidized phosphatidylcholines and polypeptides. *J Biol Chem.* 1994;269:15274-15279.

25. Shimaoka T, Kume N, Minami M, et al. Molecular cloning of a novel scavenger receptor for oxidized low density lipoprotein, SR-PSOX, on macrophages. *J Biol Chem.* 2000;275:40663–40666.
26. Grossniklaus HE, Ling JX, Wallace TM, et al. Macrophage and retinal pigment epithelium expression of angiogenic cytokines in choroidal neovascularization. *Mol Vis.* 2002;8:119–126.
27. Suzuki M, Kamei M, Itabe H, et al. Oxidized phospholipids in the macula increased with age and in eyes with age-related macular degeneration. *Mol Vis.* In press.
28. van der Schaft TL, Mooy CM, de Bruijn WC, de Jong PT. Early stages of age-related macular degeneration: an immunofluorescence and electron microscopy study. *Br J Ophthalmol.* 1993;77:657–661.
29. Chang MK, Binder CJ, Torzewski M, Witztum JL. C-reactive protein binds to both oxidized LDL and apoptotic cells through recognition of a common ligand: phosphorylcholine of oxidized phospholipids. *Proc Natl Acad Sci USA.* 2002;99:13043–13048.
30. Hazen SL, Chisolm GM. Oxidized phosphatidylcholines: pattern recognition ligands for multiple pathways of the innate immune response. *Proc Natl Acad Sci USA.* 2002;99:12515–12517.
31. Meuwissen M, van der Wal AC, Niessen HW, et al. Colocalisation of intraplaque C reactive protein, complement, oxidised low density lipoprotein, and macrophages in stable and unstable angina and acute myocardial infarction. *J Clin Pathol.* 2006;59:196–201.
32. Hageman GS, Anderson DH, Johnson LV, et al. A common haplotype in the complement regulatory gene factor H (HF1/CFH) predisposes individuals to age-related macular degeneration. *Proc Natl Acad Sci USA.* 2005;102:7227–7232.
33. Klein RJ, Zeiss C, Chew EY, et al. Complement factor H polymorphism in age-related macular degeneration. *Science.* 2005;308:385–389.
34. Haines JL, Hauser MA, Schmidt S, et al. Complement factor H variant increases the risk of age-related macular degeneration. *Science.* 2005;308:419–421.
35. Edwards AO, Ritter R III, Abel KJ, Manning A, Panhuysen C, Farrer LA. Complement factor H polymorphism and age-related macular degeneration. *Science.* 2005;308:421–424.
36. Moriwaki H, Kume N, Sawamura T, et al. Ligand specificity of LOX-1, a novel endothelial receptor for oxidized low density lipoprotein. *Arterioscler Thromb Vasc Biol.* 1998;18:1541–1547.
37. Bressler NM, Bressler SB, Congdon NG, et al. Potential public health impact of Age-Related Eye Disease Study results: AREDS report no. 11. *Arch Ophthalmol.* 2003;121:1621–1624.